

NASA TECHNICAL
MEMORANDUM



NASA TM X-1845

NASA TM X-1845

CASE FILE
COPY

STABILITY AND PERFORMANCE
CHARACTERISTICS OF SEVERAL HYDRAZINE
AND NITROGEN TETROXIDE HOT GAS
GENERATORS FOR LARGE SCALE
SUPERSONIC COMBUSTOR TESTING

by John P. Wanbainen and David W. Vincent

Lewis Research Center

Cleveland, Ohio

STABILITY AND PERFORMANCE CHARACTERISTICS OF SEVERAL
HYDRAZINE AND NITROGEN TETROXIDE HOT GAS GENERATORS
FOR LARGE SCALE SUPERSONIC COMBUSTOR TESTING

By John P. Wanhainen and David W. Vincent

Lewis Research Center
Cleveland, Ohio

NATIONAL AERONAUTICS AND SPACE ADMINISTRATION

For sale by the Clearinghouse for Federal Scientific and Technical Information
Springfield, Virginia 22151 - CFSTI price \$3.00

ABSTRACT

Performance and stability characteristics of seven different injectors utilizing injection types of like-on-like doublet elements, a combination of like-on-like doublet and showerhead elements, oxidant-fuel-oxidant triplet elements and a combination of pentad and triplet elements were investigated in 20 000-lb (89-kN) thrust engines. A baffle configuration and two different liner configurations were employed to provide additional stability margin to the basic combustors. The like-on-like doublet or the like-on-like doublet and shower-head element injectors were the only configurations that were statically stable. Acoustic liners provided some dynamic stability.

STABILITY AND PERFORMANCE CHARACTERISTICS OF SEVERAL
HYDRAZINE AND NITROGEN TETROXIDE HOT GAS GENERATORS
FOR LARGE SCALE SUPERSONIC COMBUSTOR TESTING

by John P. Wanhainen and David W. Vincent

Lewis Research Center

SUMMARY

The Lewis Research Center has conducted an experimental investigation to determine the acoustic mode stability and performance characteristics of several hydrazine and nitrogen tetroxide rocket combustors. The combustors were planned to be used as hot gas generators in a hypersonic combustion facility, so the tests were limited to an oxidant-fuel ratio of 3 at which the exhaust products simulate the composition of air. The tests were conducted at a nominal chamber pressure of 300 psia (2070 kN/m^2) and a nominal thrust level of 20 000 pounds (89 kN). Seven different injectors utilizing injection types of like-on-like doublet elements, combination of like-on-like doublet elements and showerhead elements, oxidant-fuel-oxidant triplet elements and combination of pentad and triplet elements were used in the investigation.

Injector configurations which utilized like-on-like doublet elements or like-on-like fuel doublet elements and showerhead oxidizer elements were the only configurations that were statically stable. With the use of acoustic liners, the stability margin of the statically stable combustors could be improved. A characteristic exhaust velocity efficiency of $96\frac{1}{2}$ percent was achieved with a like-on-like doublet element injector.

INTRODUCTION

Ground simulation of inlet conditions for air breathing propulsion devices has become increasingly more difficult with increases in flight Mach number. Pressure and particularly temperature requirements to simulate hypersonic flight inlet conditions exceed the supply capabilities of most existing facilities. One technique presently under consideration at the Lewis Research Center to simulate inlet conditions for hypersonic flight is

to use the exhaust products of a rocket burning hydrazine and nitrogen tetroxide propellants (ref. 1). When burned at an oxidant-fuel ratio of about 3, the combustion products approximate the composition of air in which part of the nitrogen is replaced by water vapor. The theoretical combustion products consist of 39 percent water vapor, 39 percent nitrogen, and 21 percent oxygen.

Preliminary rocket tests (ref. 1) determined that the gas generator combustor concept was feasible, however, the combustors were plagued with acoustical-mode combustion instability. The purpose of this study was to evaluate the stability and performance characteristics of several different types of injectors and select the most stable and efficient configuration for use in the Center's hypersonic burner investigation. The injector types tested included: a triplet injector, an intersecting fan (like-on-like) doublet injector, a parallel-fan (like-on-like) doublet injector, a like-on-like doublet and shower-head combination injector, and a pentad-triplet combination injector. The like-on-like doublet element injectors were fabricated for this investigation and patterned after small scale work reported in reference 2. The unlike-impingement type injectors were existing configurations used previously in other programs with 50 percent UDMH-50 percent N_2H_4 and N_2O_4 propellants. A baffle configuration and two different acoustic liner configurations were also employed to provide additional stability margin to the basic combustors. Tests evaluating the baffle and liners, however, were limited to only the statically stable injectors.

The experiments were conducted in 20 000-pound (89-kN) thrust combustors operating at a nominal chamber pressure of 300 psi (2070 kN/m²). The oxidant-fuel ratio was held constant at a nominal value of 3.0. Stability rating of the statically stable combustor configurations was accomplished by subjecting the combustor to radially directed pressure pulses generated by various size nitrocellulose charges.

APPARATUS

Facility

The Rocket Engine Test Facility of the Lewis Research Center is a 50 000-pound (222.5-kN) thrust, sea level stand equipped with an exhaust gas muffler and scrubber (fig. 1). The facility utilized a pressurized propellant system to deliver the propellants to the combustor. The propellant tanks consisted of a 55-cubic-foot (1.56-m³) fuel tank and a 55-cubic-foot (1.56-m³) oxidizer tank.

The combustor was mounted on the thrust stand to fire vertically downward into the scrubber where the exhaust gases were sprayed with water at rates to 50 000 gallons per minute (189 m³/min) for the purposes of cooling and sound suppression. Prior to being discharged into the atmosphere, the cooled exhaust gases were further sprayed with ammonia to reduce the unburned nitrogen tetroxide to ammonium nitrate. The amount of

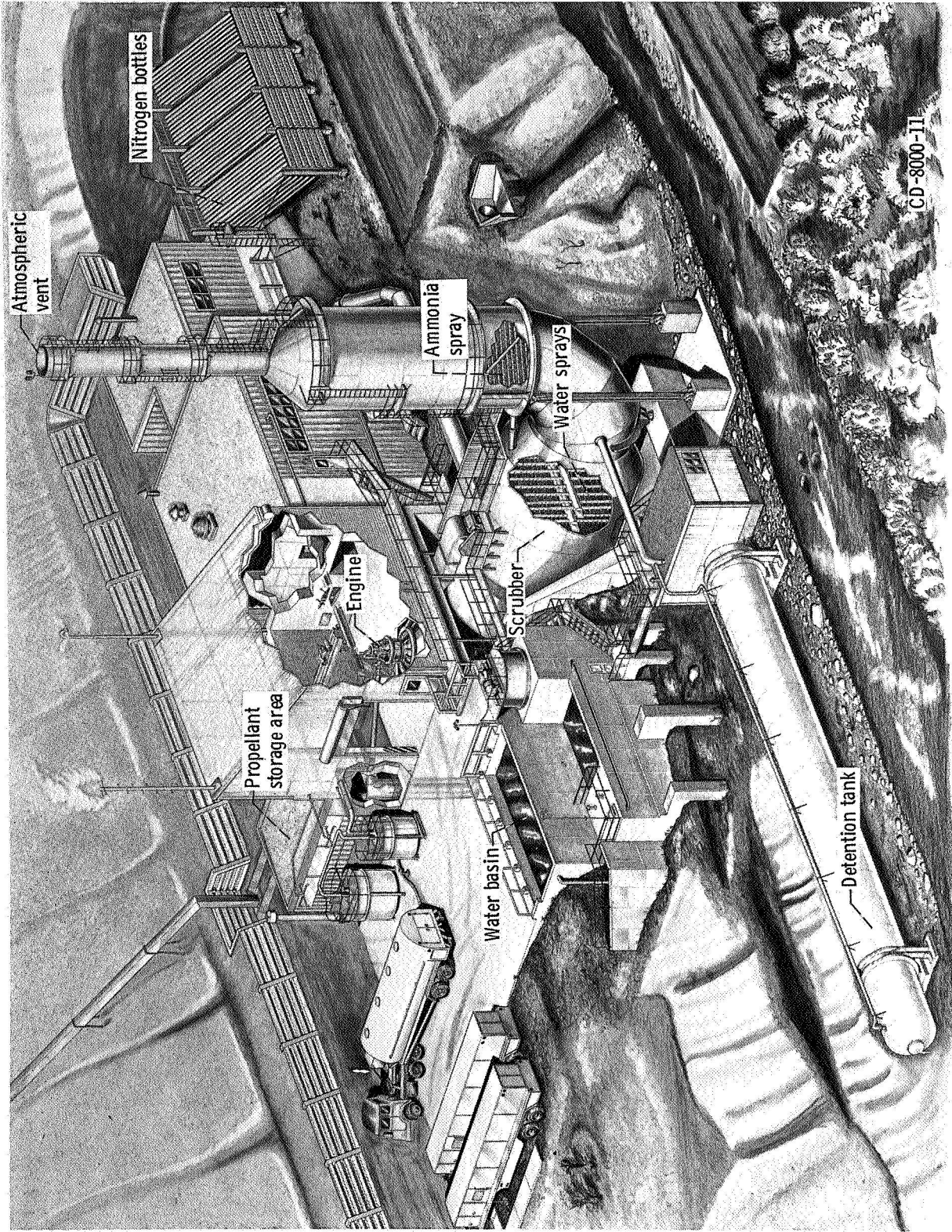


Figure 1. - Test facility.

ammonia used was 1-pound per pound (1-kg/kg) of unburned oxidizer. The exhaust gas cooling water was collected in a detention tank (fig. 1) and neutralized with sodium hydroxide. The pressurization gases from the propellant tanks were also neutralized before venting into the atmosphere. In the case of the oxidizer, the vent discharged into the detention tank and the fuel vent discharged into a water basin containing calcium hypochlorite or hydrogen peroxide.

The facility was operated remotely from a control room located 2000 feet (610 m) from the facility. In addition to a central data recording system, the facility was equipped with several direct reading oscillographs and a magnetic type recorder to record test results.

COMBUSTORS

To minimize test hardware costs, heat-sink versions of the water cooled gas generators to be used in the hypersonic combustion facility were used to evaluate the injector stability characteristics. A cross-sectional view of a typical combustor which consisted

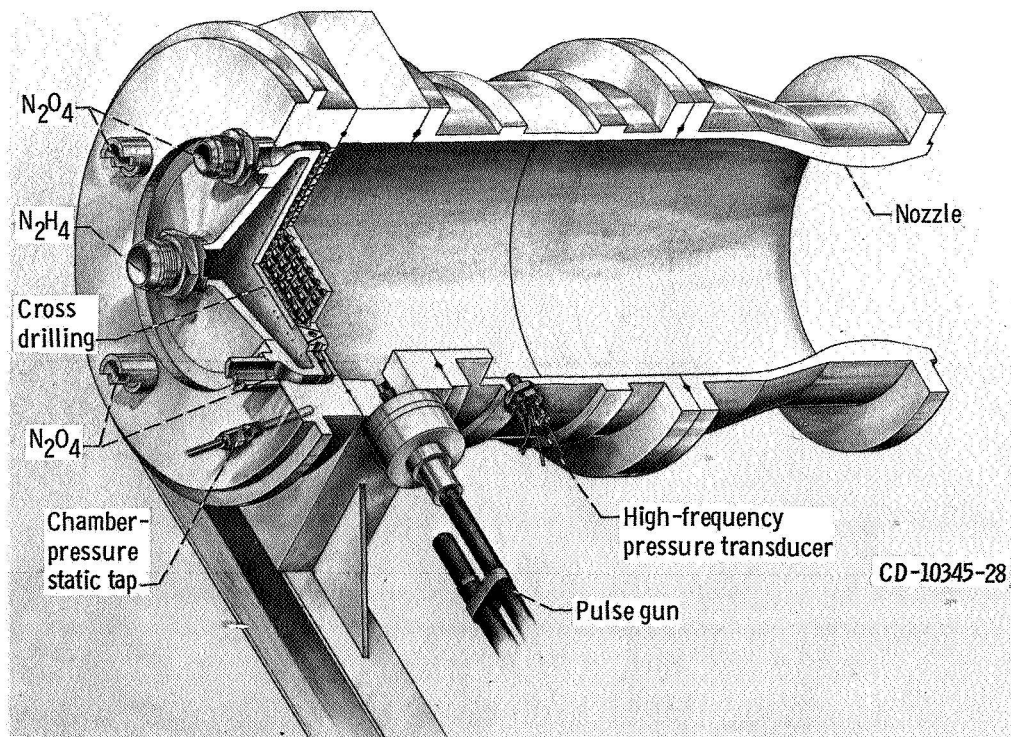


Figure 2 - Sectional view of heat-sink rocket engine (gas generator).

of an injector, a 10.78-inch (27.4-cm) cylindrical thrust chamber and a 1.9 contraction ratio exhaust nozzle, is shown in figure 2. The expansion ratio of the nozzle which was 1.3 was selected for the convenience of operation since it had no effect on combustion stability. The inner surfaces of the mild steel combustion chambers and nozzles were coated with a 0.012-inch (0.030-cm) thick layer of Nichrome and a 0.018-inch (0.046-cm) thick layer of zirconium oxide to reduce heat transfer into the metal. This coating allowed a test duration of 3 seconds without damage to the combustor walls.

Injectors

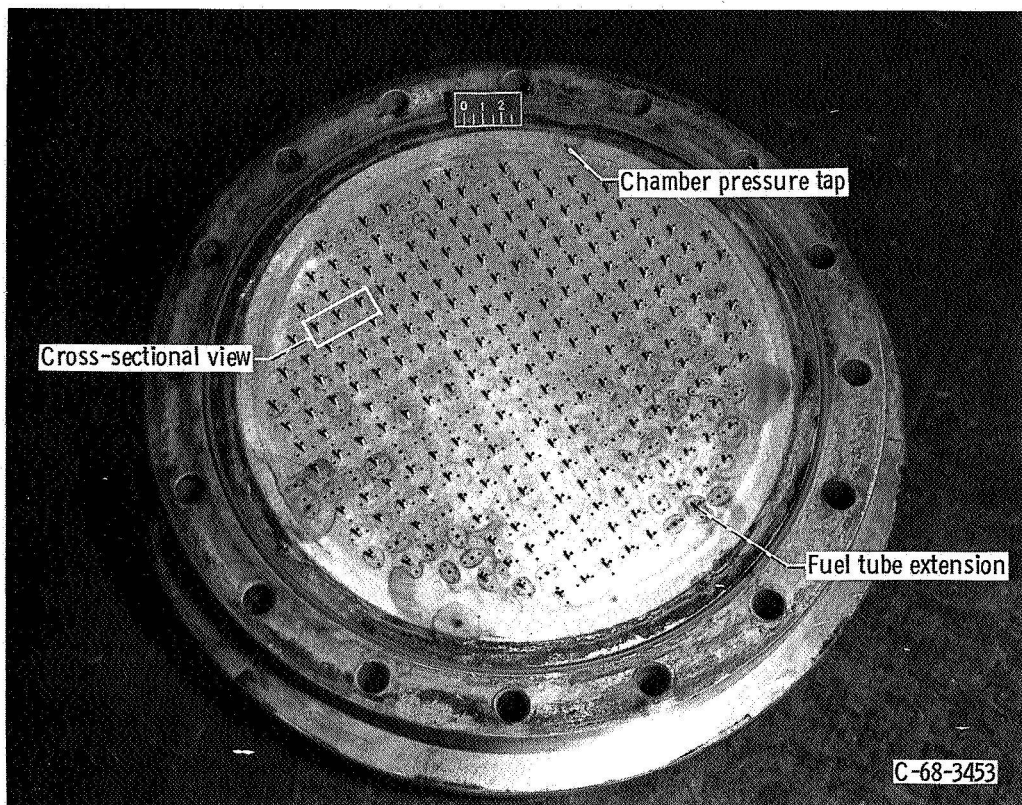
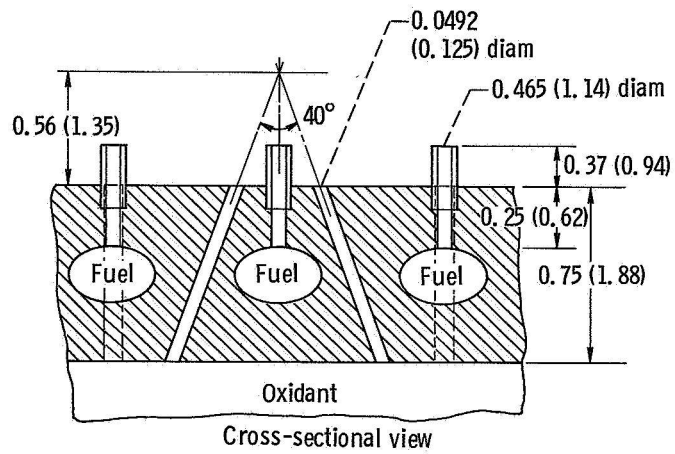
A total of seven flat-faced aluminum alloy injectors of the following configurations were tested:

- (1) Injector A, 268 oxidant-fuel-oxidant triplet elements (fig. 3(a))
- (2) Injector B, 387 oxidant doublet elements and 129 fuel doublet elements with fuel fans intersecting with oxidant fans (fig. 3(b))
- (3) Injector C, 144 oxidant doublet elements, 4 oxidant shower-head elements and 52 fuel doublet elements, elements arranged to form parallel fans (fig. 3(c))
- (4) Injector D, 252 oxidant doublet elements, 96 fuel doublet element and 32 fuel shower-head elements with elements arranged to form parallel fans (fig. 3(d))
- (5) Injector E, 980 oxidant shower-head elements and 96 fuel doublet elements (fig. 3(e))
- (6) Injector F, 112 oxidant-fuel-oxidant triplet elements and 188 oxidant-on-fuel pentad elements (fig. 3(f))
- (7) Injector G, 101 fuel-oxidant-fuel triplet elements (fig. 3(g))

With the exception of the last configuration, the injection orifices were circular and the faceplate was cooled by flow of the oxidizer through cross drilled passages. The 101 element triplet injector (fig. 3(g)) incorporated rectangular injection apertures, in addition to circular ones, in an attempt to provide more stability through increased propellant stream hydraulic rigidity to a tangential mode pressure wave. The faceplate was fuel cooled. Other injector details such as injection orifice sizes, impingement angles, and impingement distances may be found by referring to the injector cross sectional views (fig. 3) and table I.

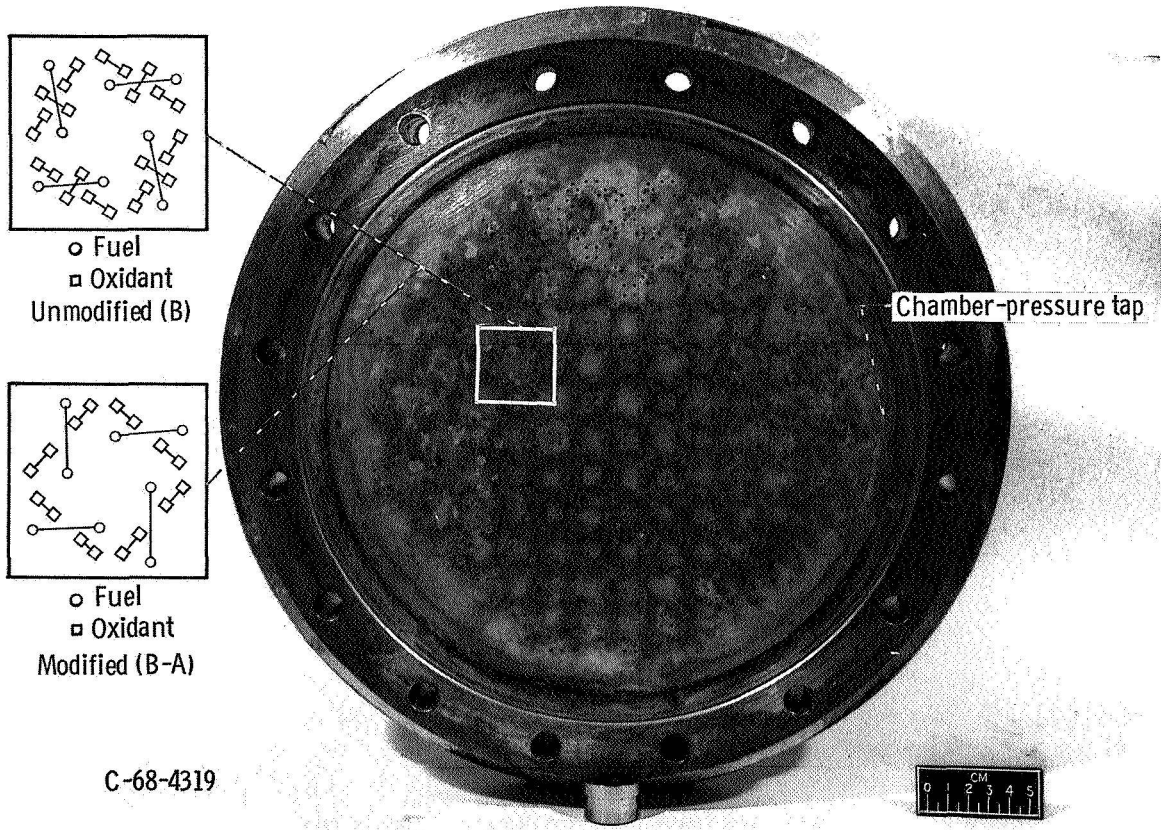
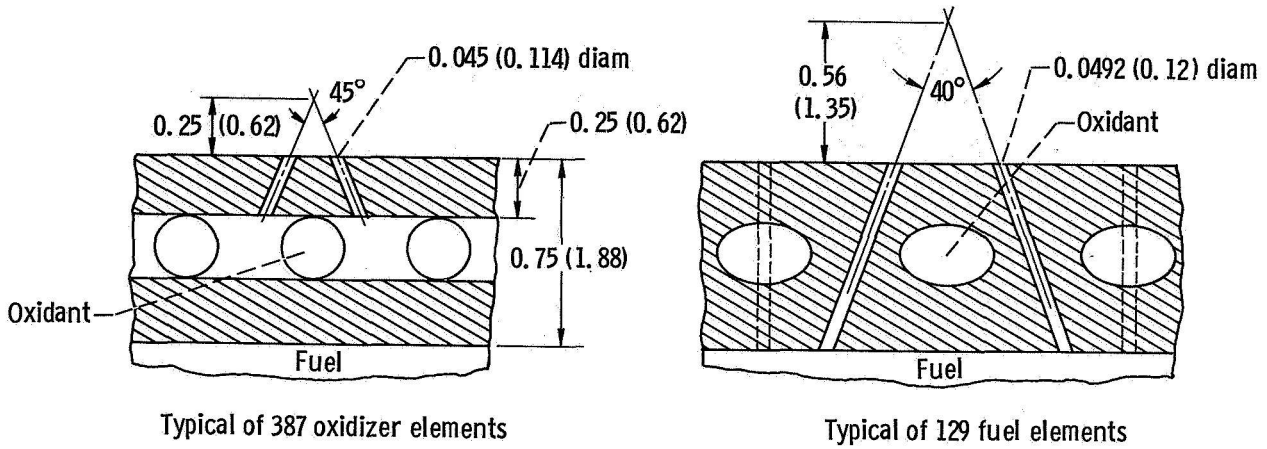
Pulse Gun

The pulse gun which was used as a stability rating device was mounted into the cylindrical chamber section as shown in figure 4. The radial injection port was used for this investigation. The pulse gun chamber section was generally located immediately



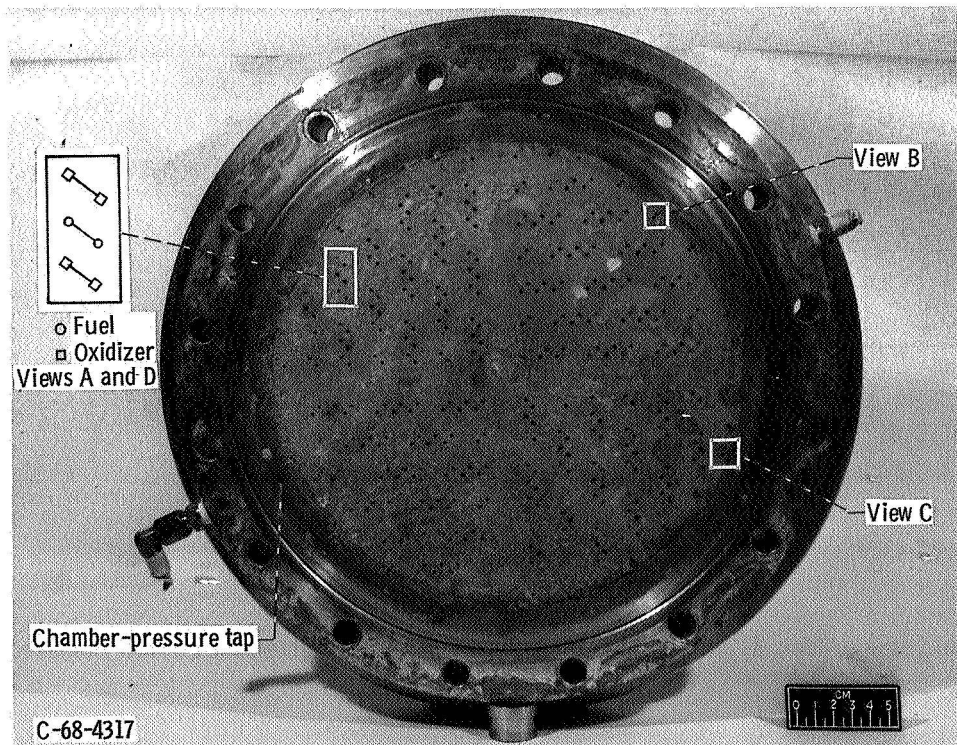
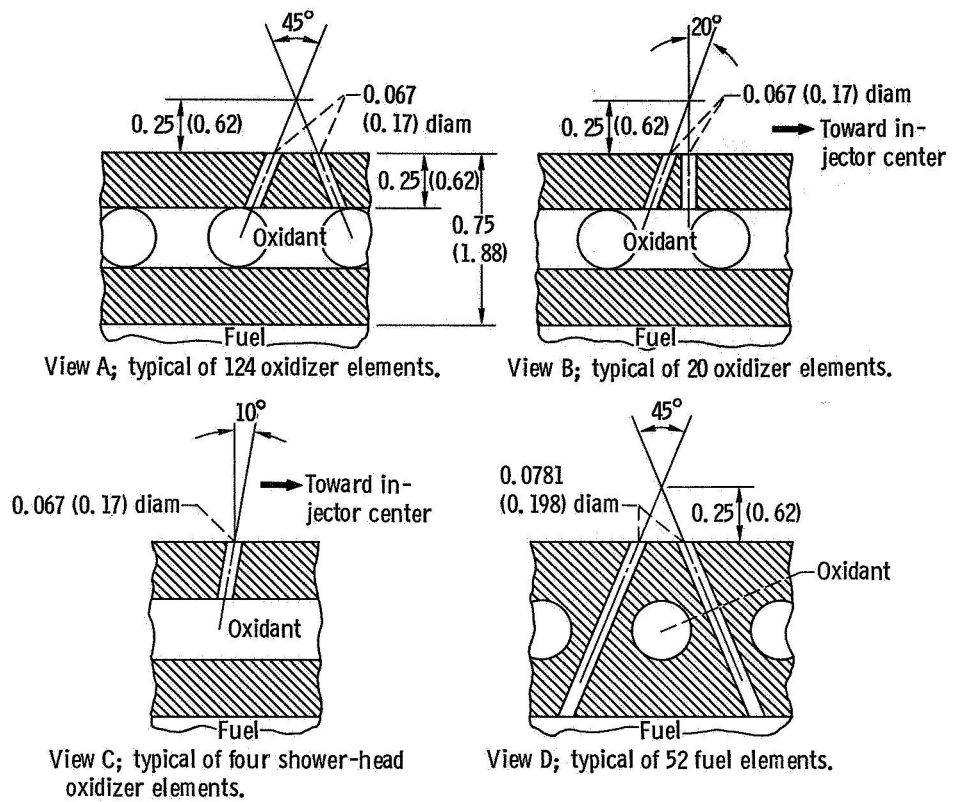
(a) Configuration A; 268-element oxidant-fuel-oxidant triplet. (All dimensions are in inches (cm).)

Figure 3. - Faceplate and cross-sectional views of injector configurations.



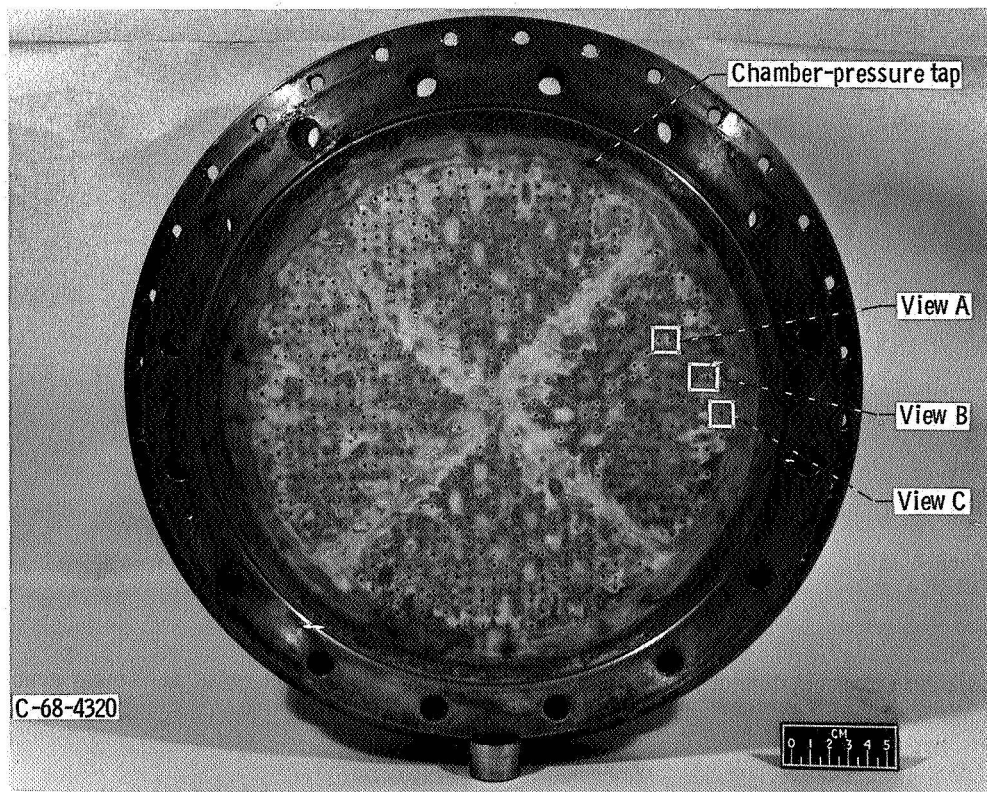
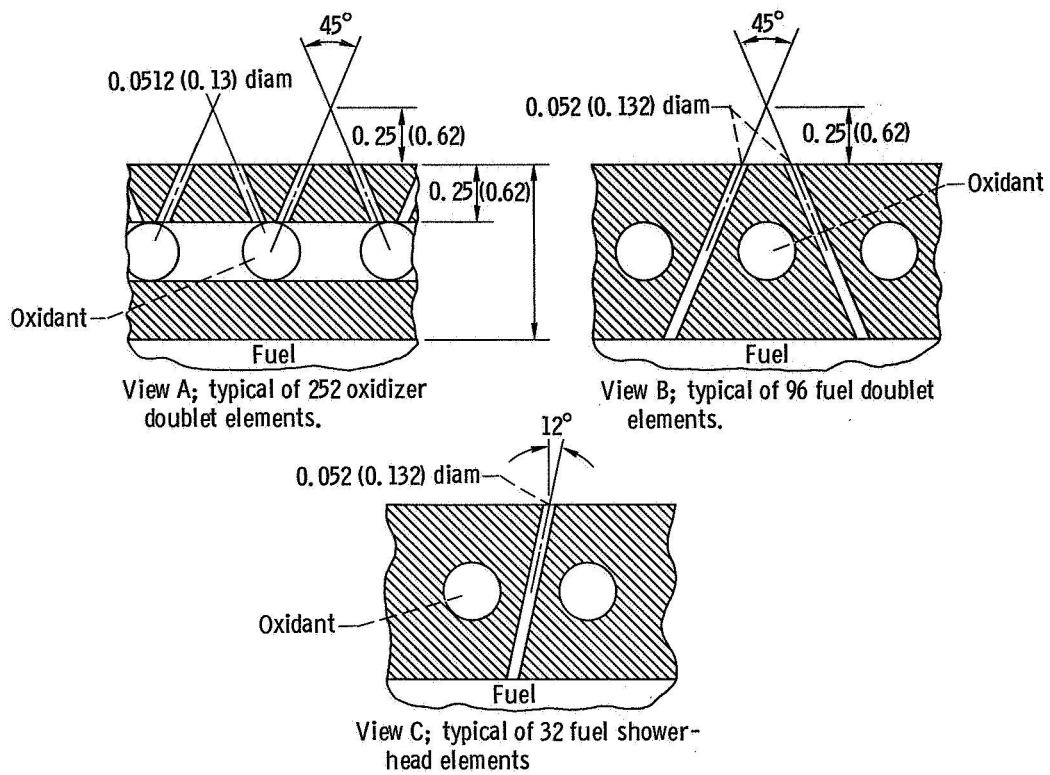
(b) Configuration B; intersecting fan doublet. (All linear dimensions are in inches (cm).)

Figure 3. - Continued.



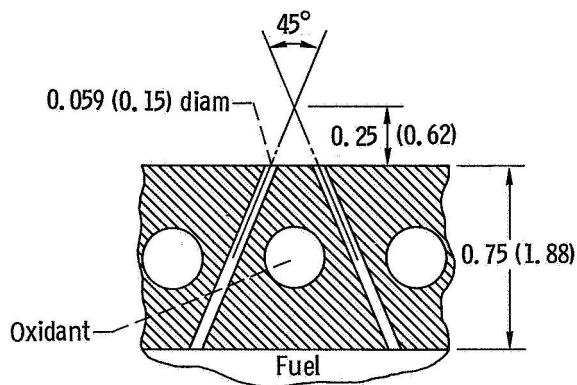
(c) Configuration C; parallel fan like-on-like doublet. (All linear dimensions in inches (cm).)

Figure 3. - Continued.

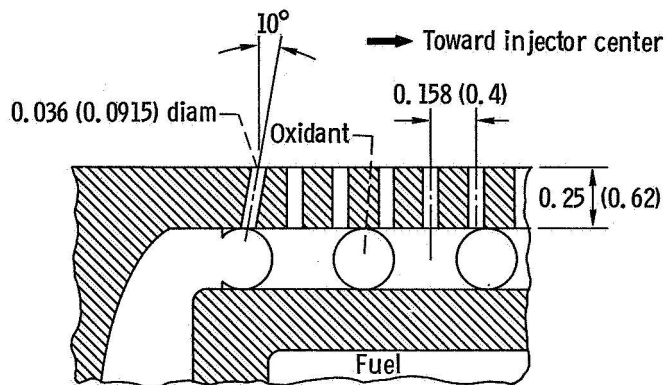


(d) Configuration D; parallel fan, like-on-like doublet. (All linear dimensions in inches (cm).)

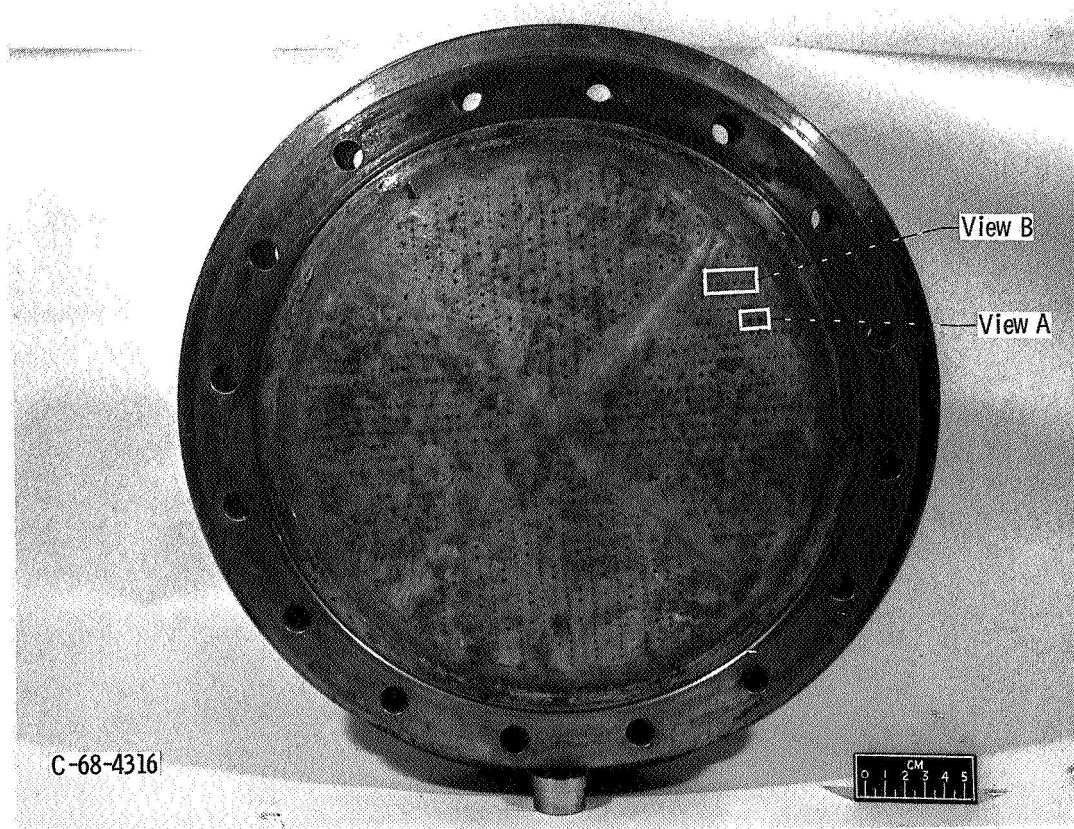
Figure 3. - Continued.



View A; typical of 96 fuel doublet elements.

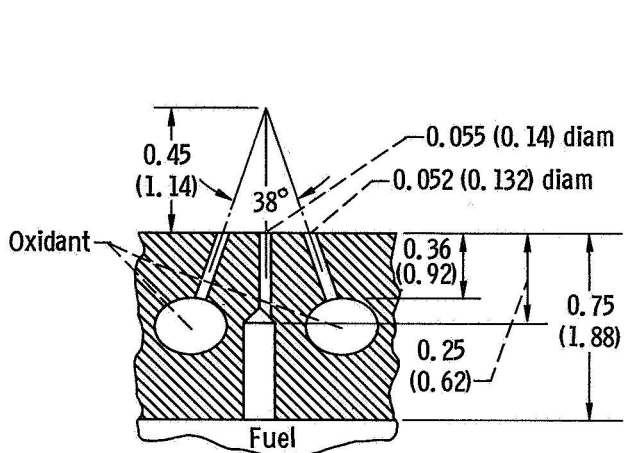


View B; typical of 980 showerhead oxidizer elements.

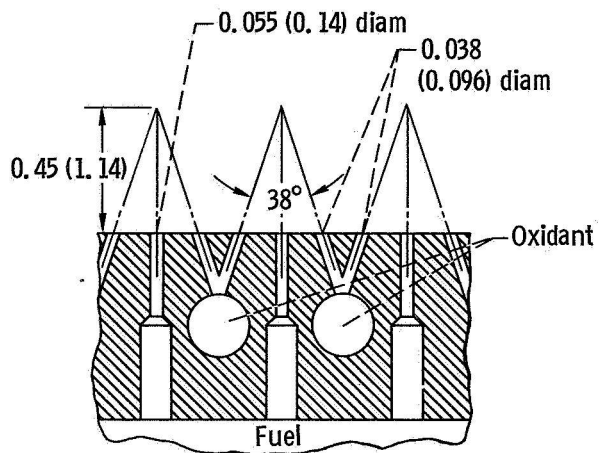


(e) Configuration E; combination of fuel doublet and showerhead oxidizer elements. (All linear dimensions are in inches (cm).)

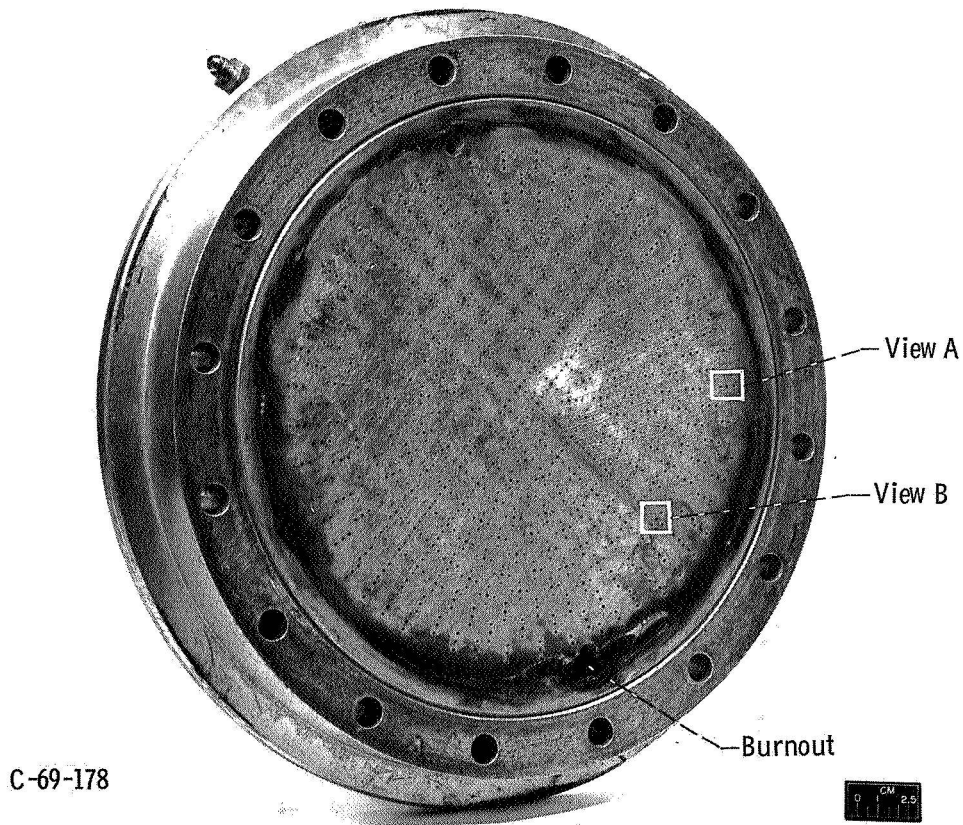
Figure 3. - Continued.



View A; typical of 112 triplet elements.

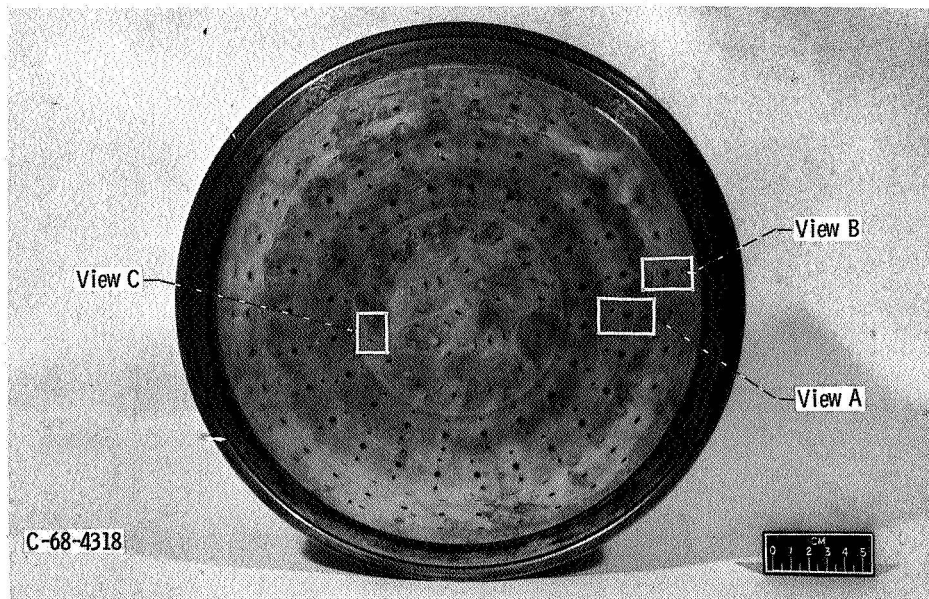
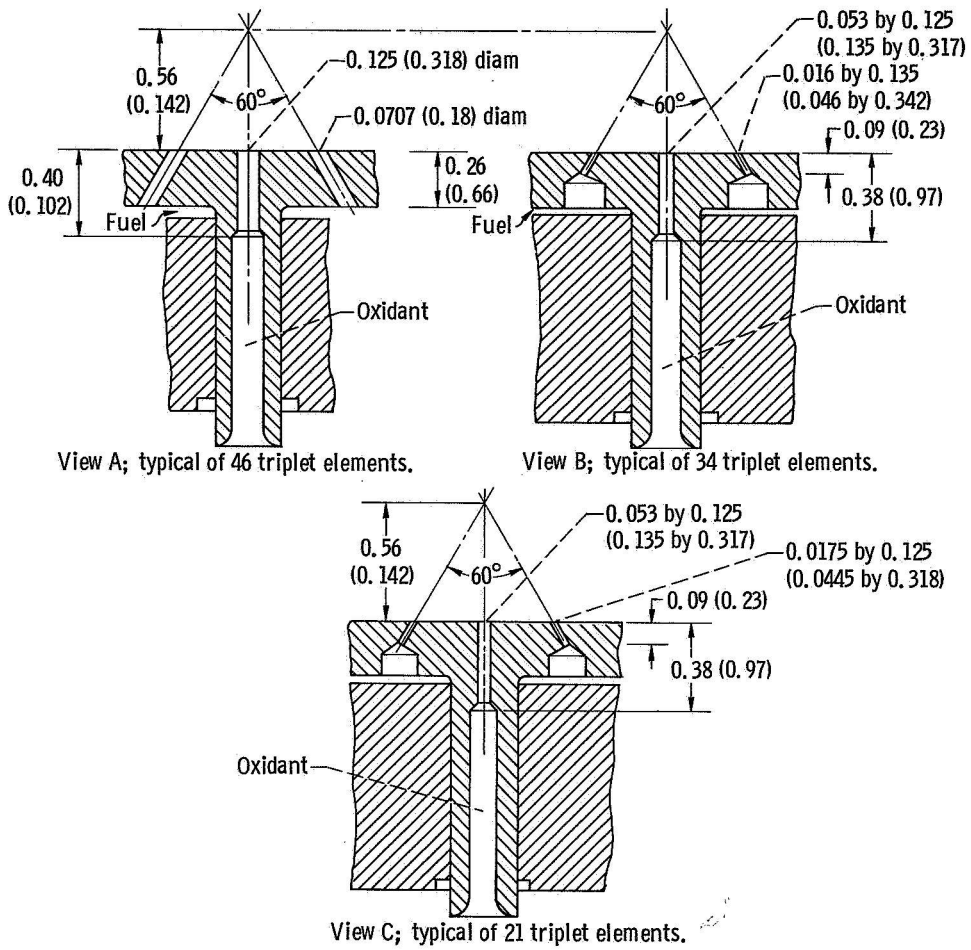


View B; typical of 188 pentad element.



(f) Configuration F; fuel-oxidizer-fuel triplets and fuel on oxidizer pentads. (All linear dimensions are in inches (cm).)

Figure 3. - Continued.



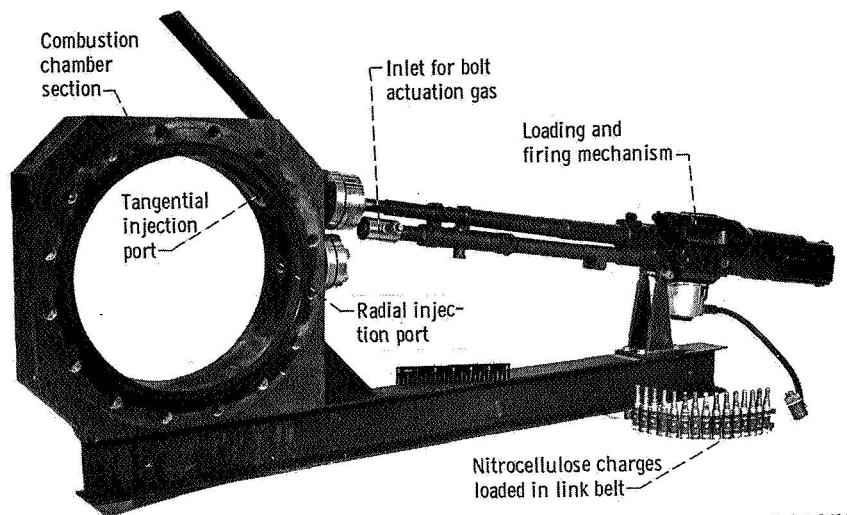
(g) Configuration G utilizing both circular and slit orifices. (All linear dimensions in inches (cm).)

Figure 3. - Concluded.

TABLE I. - INJECTOR CONFIGURATIONS

Injector	Pattern configuration	Total number of oxidant orifices		Oxidant orifice diameter		Total number of fuel orifices	Fuel orifice diameter		Injection areas				Injection velocities ^a					
											Oxidant		Fuel		Oxidant		Fuel	
		in.	cm	in.	cm		in. ²	cm ²	in. ²	cm ²	in. ²	cm ²	ft/sec	m/sec	ft/sec	m/sec		
A	Oxidant-fuel-oxidant triplet (fuel orifice extended 0.37 in. (0.94 cm))	536		0.0492	0.125	268	0.0485	1.14	1.108	7.15	0.455	2.93	108	32.9	126	38.4		
B	Like doublets with fans intersecting	774		0.045	0.114	258	0.0492	0.12	1.23	7.93	0.49	3.16	98	29.9	117	35.7		
B-A	Modification: closed intersecting oxidant doublets	516		0.045	0.114	258	0.0492	0.12	0.82	5.28	0.49	3.16	147	44.8	117	35.7		
C	Like doublets with parallel fans	292		0.067	0.17	104	0.0781	0.198	1.03	6.64	0.497	3.21	117	35.7	115	35.1		
D	Like doublets with parallel fans	504		0.0512	0.13	224	0.052	0.132	1.036	6.67	0.475	3.06	116	35.4	121	36.9		
E	Oxidant shower-heads with fuel doublets	980		0.036	0.0915	192	0.0591	0.15	0.996	6.42	0.526	3.39	121	36.9	190	33.3		
F	Oxidant-fuel-oxidant triplets with oxidant on fuel pentads	224 752		0.052 .038	0.132 .096	300	0.055	0.14	1.327	8.51	0.712	4.58	90	27.4	81	24.7		
G	Fuel-oxidant-fuel triplets with slot and circular shape orifice combination	46 55		0.125 .053 x .125	0.318 .135 x .317	92 42 68	0.0707 .0175 x .125 .016 x .135	0.18 .0445 x .318 .046 x .342	0.919 5.93	0.603 4.89	131 40	95 29						

^aPropellant temperature, 75° F (99 K); oxidant weight flow, 75 lb/sec (34 kg/sec); fuel weight flow, 25 lb/sec (11.35 kg/sec).



C-66-2609

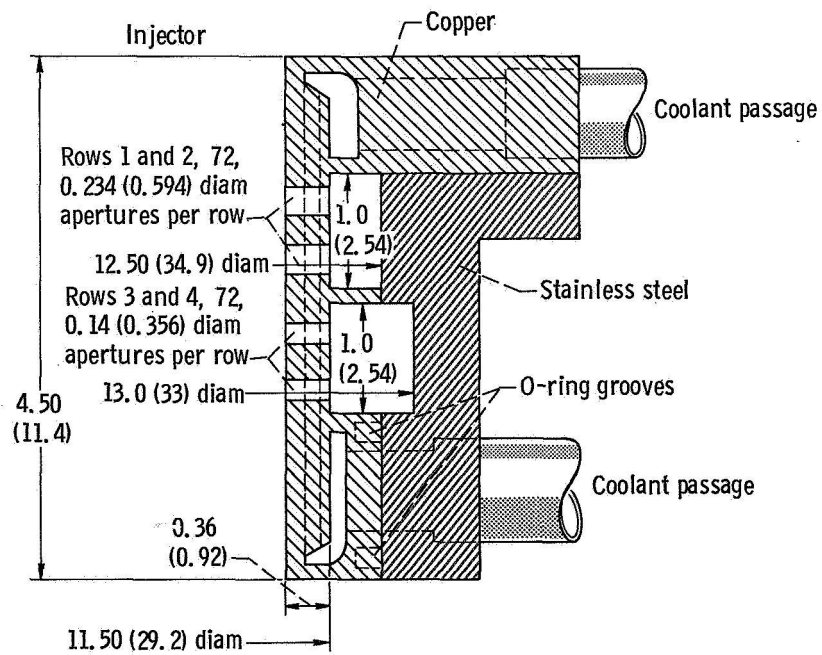
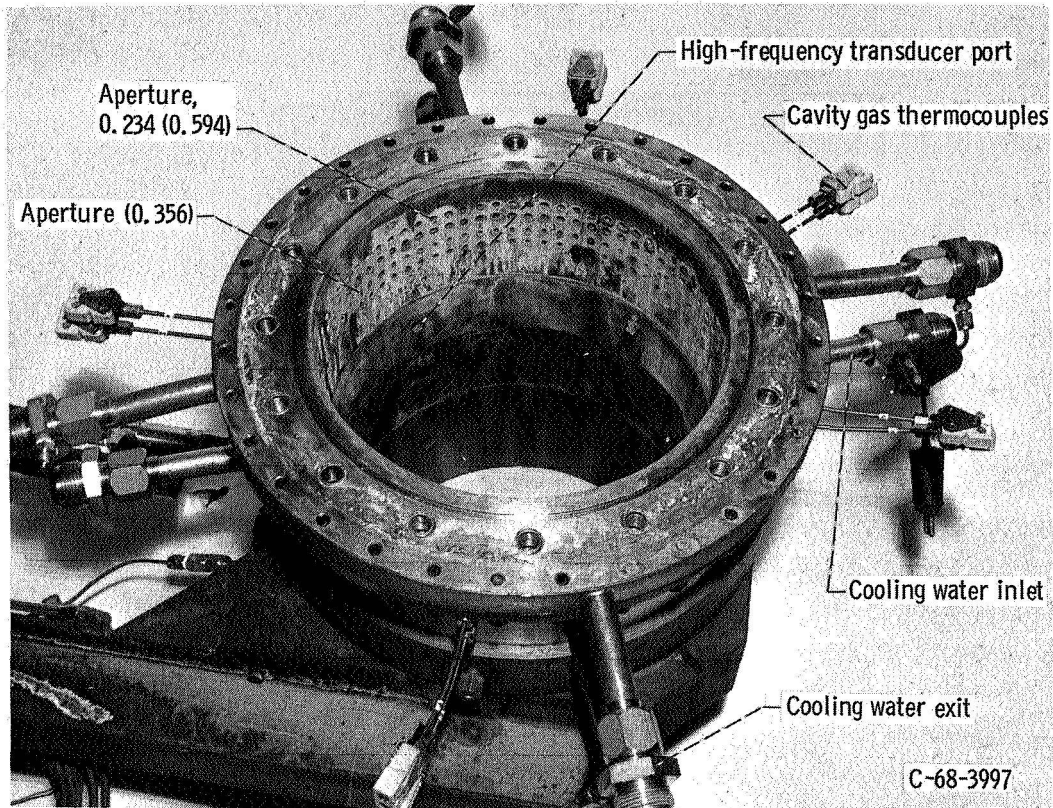
Figure 4. - Machine gun mounted to chamber section.

downstream of the injector. In those tests where an acoustic liner or baffle assembly was mounted adjacent to the injector, the chamber section with gun port was moved immediately downstream of the screech suppression devices.

The pulse gun consisted of a modified 30-caliber (7.62-mm) machine gun with blank cartridges containing several different charge sizes of nitrocellulose. Charge sizes ranged from 18.5 grains (1.2 grams) to a maximum of 39 grains (2.53 grams). The maximum limit was imposed by the cartridge volume. Because of the high chamber pressure (300 psia or 2070 kN/m²) it was necessary to insert a check valve in the gun barrel to seal against chamber pressure leakage between pulses. The advantages, a typical firing cycle and other operating details of this type pulse gun are described in reference 3.

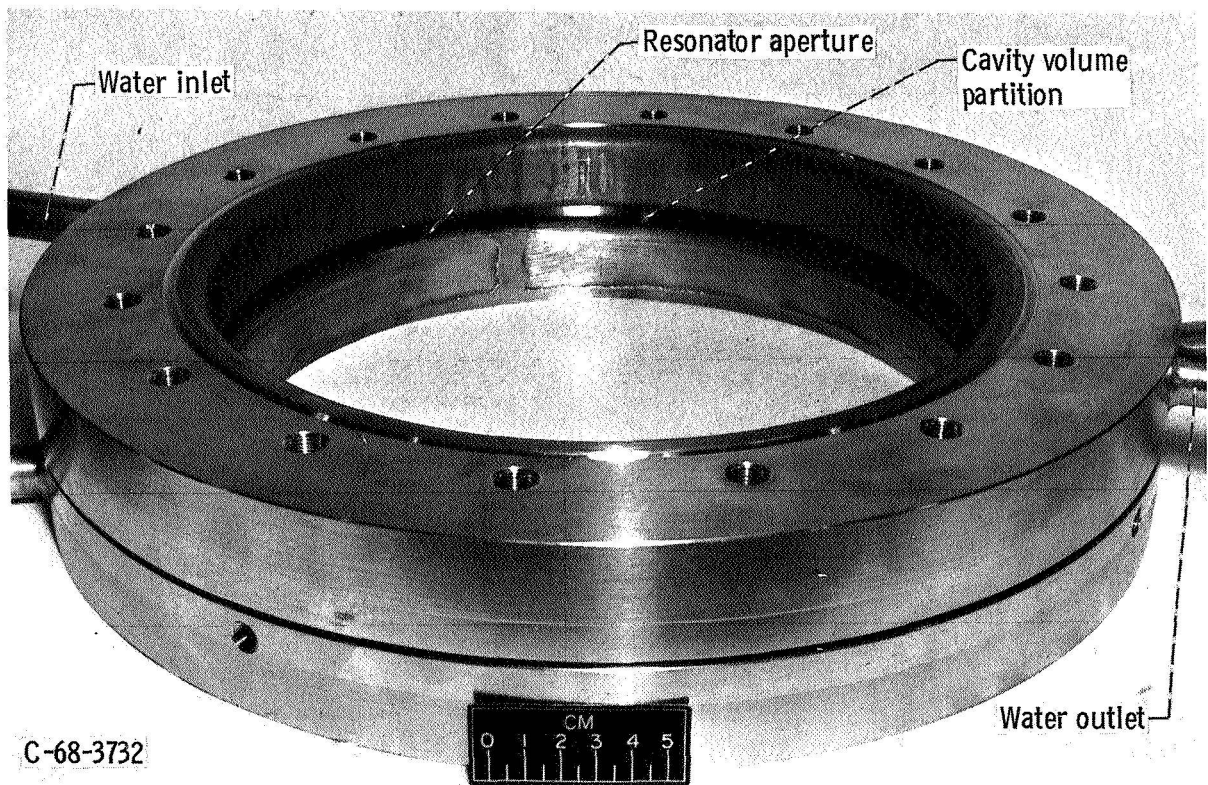
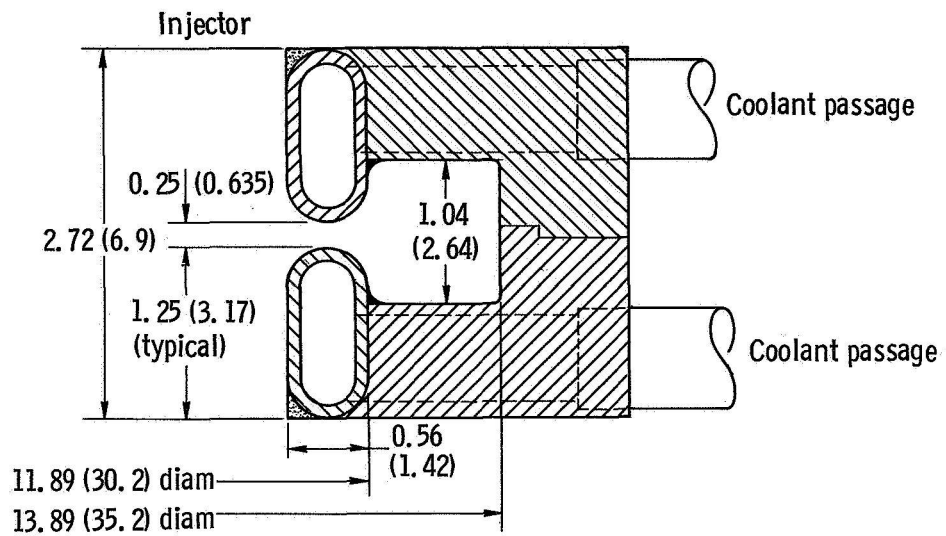
Screech Suppression Devices

Photographs and cross sectional views of a water cooled, perforated plate, circular aperture acoustic liner and a water cooled, circumferential slot acoustic liner tested are shown in figure 5. The liners were fabricated from oxygen free, high conducting copper. Heat sink hardware was not used because of the possibility of a change in liner cavity gas temperature and therefore liner resonant frequency with uncooled hardware. The circular aperture liner (fig. 5(a)) had a total of 288 apertures in four circumferential rows: two upstream rows with apertures 0.234 inch (5.94 mm) in diameter and two rows with apertures 0.140 inch (3.55 mm) in diameter. As shown in figure 5(a) the liner backing volume was divided into two compartments by a circumferential partition so that each



(a) Water-cooled circular aperture acoustic liner. (All linear dimensions are in inches (cm).)

Figure 5. - Acoustic liners.



(b) Water-cooled circumferential slot acoustic liner. (All linear dimensions are in inches (cm).)

Figure 5. - Concluded.

part (two aperture rows) could be tuned independently. The design frequencies for the circular aperture liner were 2200 and 3800 hertz which correspond to the first and second tangential modes for the chamber at the operating conditions tested. For design purposes, the liner gas temperature was assumed to be between 1440° R (800 K) and 2520° R (1400 K) and the aperture effective length was assumed to be equal to the liner thickness plus 0.375 times the effective length correction factor (ref. 4).

The circumferential slit liner was a very simple design consisting of two flattened pieces of copper tubing separated 0.25-inch (6.35-mm) to form the resonator aperture (fig. 5(b)). The design resonant frequency of the liner was 2200 hertz. The liner was designed using equations and empirical relations from references 5 and 6.

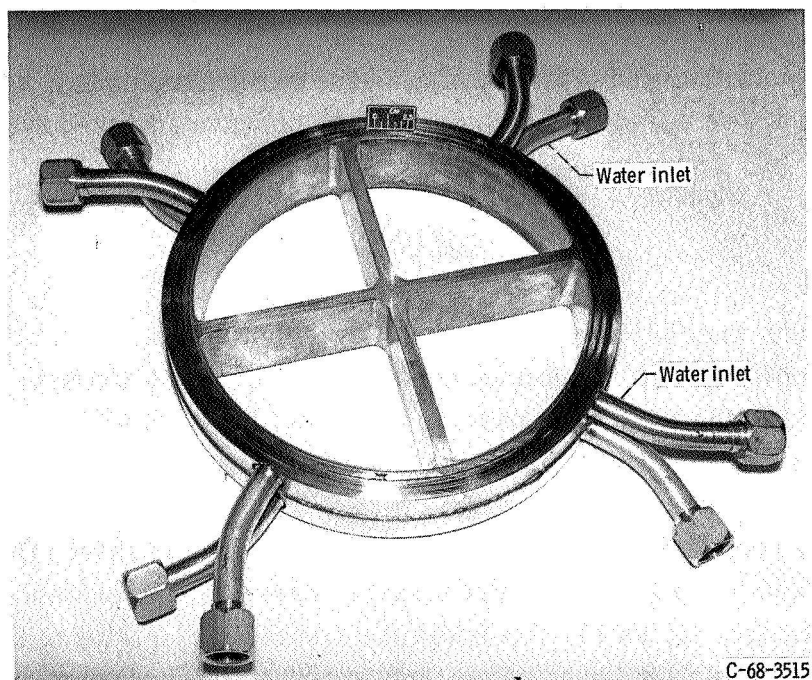


Figure 6. - Water-cooled baffle.

A photograph of the four-spoke, water-cooled baffle is shown in figure 6. The baffle was $2\frac{1}{4}$ inches (5.72 cm) in length and fabricated from oxygen-free, high-conducting copper. The cooling water entered the downstream half of the baffle legs from a circumferential manifold, flowed to a common manifold at the baffle leg intersection and exited through the upstream half of the baffle. The design cooling water flow rate was 24 pounds per second (10.9 kg/sec).

Instrumentation

Combustor operating parameters were recorded on the Center's automatic digital data recording system and on direct reading instruments in the control room of the facility for monitoring during tests. Strain gage transducers were used to measure steady state pressures. Propellant weight flows were determined with turbine-type flowmeters. The pressure transducers were calibrated immediately prior to data acquisition by an electrical two-step calibration system, which used resistances in an electrical circuit to simulate a given pressure.

Piezoelectric-type, water-cooled, flush-mounted pressure transducers were used at three locations on the thrust chamber to determine the amplitude and phase relation of the oscillatory pressure field for identification of the acoustic mode. The response characteristics of the transducers as installed were flat to within ± 10 percent to a frequency of 10 000 hertz and had a nominal resonant frequency of about 20 000 hertz. The signals from the high frequency response transducers were recorded on magnetic tape, then replayed at reduced tape speed onto an oscillograph or wave analyzer for analysis.

PROCEDURE

Program timers were utilized to sequence propellant valves. About 10 seconds prior to oxidizer valve opening, the injector was purged with gaseous nitrogen. The purge pressure measured in the injector manifolds was about 50 psi (345 kN/m^2). The hydrazine fire valve was scheduled to open approximately 1/2 second after the oxidizer fire valve. The initial operating conditions were selected by presetting the fire valves. Approximately 1/2 second after rated chamber pressure was attained, propellant flow rates were regulated (maintaining a given chamber pressure and oxidant-fuel ratio constant throughout the test) by an electro-hydraulic controller. Firing of the machine gun for stability rating was scheduled to commence at about 1 second after rated conditions were reached. The gun was discharged a total of six times at 0.3-second intervals during a test. Shutting down the engine was accomplished by closing both propellant valves simultaneously and then purging the injector of propellants with gaseous nitrogen. A water flush was also used on the fuel side to insure that the injector was completely purged of hydrazine.

RESULTS AND DISCUSSION

As mentioned in the section INTRODUCTION, the combustors evaluated in this investigation were candidates for use as gas generators in a hypersonic combustion facility,

thus, the tests were limited to operating conditions that would provide the proper gas constituents in the exhaust products. Theoretically, at an oxidant-fuel ratio of 3, the exhaust products simulate air in which water vapor replaces part of the nitrogen. A few tests were conducted at other oxidant-fuel ratios and chamber pressures other than 300 psia (2070 kN/m^2) with the most stable combustor to insure that slight changes in operating conditions from the nominal would not significantly affect the stability characteristics.

As noted earlier, a pulse gun discharging radially into the thrust chamber was used as a stability rating device. The location of the pulse gun with respect to the injector was maintained constant for all tests evaluating stability of the basic combustor, thus, a direct comparison of the stability data can be made. In those tests where an acoustic liner or a baffle was evaluated, the base line stability (without damping devices) was different from that of the basic engine because of a different location of the pulse gun. Moving the pulse gun downstream (about 2.5 in. or 6.35 cm) of the chamber section containing the acoustic liner changed the baseline stability of injector D from less than $18\frac{1}{2}$ to $27\frac{1}{2}$ grains (1.2 to 1.78 grams) of nitrocellulose.

The experimental data recorded for each test conducted in the investigation are shown in table II. In those tests where combustion instability was encountered, the mode of the oscillation and the number of grains of nitrocellulose that induced instability are also tabulated. In addition, typical amplitude spectral density graphs are presented for each combustor during unstable operation at nominal operating conditions.

INJECTOR STABILITY AND PERFORMANCE CHARACTERISTICS

Injector configuration A: 268 element, oxidant-fuel-oxidant triplet injector. - This injector (fig. 3(a)) was an existing configuration that had previously been statically stable with 50 percent N_2H_4 - 50 percent UDMH and N_2O_4 propellant combination at oxidant-fuel ratios of 2 and below. Initial tests (ref. 1) which were conducted prior to the investigation reported herein, indicated that the configuration was spontaneously unstable with the hydrazine and N_2O_4 propellant combination. In an attempt to improve stability, the injector was modified by inserting tubes into the fuel orifices to insure proper impingement with the oxidizer streams. The tube extension was 0.37 inch (0.94 cm). This modification was found to improve stability in small scale tests reported in reference 7.

TABLE II. - EXPERIMENTAL DATA

(a) Combustors without screen suppression devices

In- jec- tor	Run	Combustor configuration	Combustor length ^a		Pulse gun position ^b		Charge infor- mation, grain (gram) where applicable	Mode	Characteristic exhaust velocity efficiency, η_c^*	Oxidant- fuel ratio, O/F	Chamber pressure		Oxidant flow rate		Fuel flow rate		Oxidant injector pressure change		Fuel injector pressure change		Remarks
			in.	cm	in.	cm					psi	kN/m^2	lbm/sec	kg/sec	lbm/sec	kg/sec	psi	kN/m^2	psi	kN/m^2	
A	3	Basic heat sink	28.4	72.1	---	----	No pulses, spon- taneous instability	(c)	η_{c96}	2.57	331	2280	73.9	33.5	28.7	13	220	1515	321	2210	
	6	Basic heat sink	20.1	51	6.6	16.75	No pulses, spon- taneous instability	IT	η_{c91}	2.78	331	2280	79.6	36.1	28.6	12.95	257	1770	360	2480	
	7	Basic heat sink	20.1	51	6.6	16.75	No pulses, spon- taneous instability	IT	$\eta_{c92.6}$	3.37	314	2165	81.4	36.9	24.1	10.9	276	1900	231	1590	
B	10	Basic heat sink	21.6	54.9	1.6	4.07	No pulses, spon- taneous instability	IT	$\eta_{c87.2}$	2.62	314	2165	76.7	34.8	29.3	13.3	188	1295	174	1200	
	22	Basic heat sink	21.6	54.9	1.6	4.07	No pulses, spon- taneous instability	IT	$\eta_{c84.3}$	2.60	222	1530	55.3	25.1	21.2	9.63	162	1117	131	903	
	23	Basic heat sink	21.6	54.9	1.6	4.07	No pulses, spon- taneous instability	IT	η_{c91}	2.54	225	1550	51.1	23.2	20.2	9.17	131	903	112	772	
B-A	45	Basic heat sink	21.6	54.9	1.6	4.07	No pulses, spon- taneous instability	IT	η_{c92}	2.67	305	2100	71.9	32.6	26.9	12.2	220	1515	---	---	
	46	Basic heat sink	21.6	54.9	1.6	4.07	No pulses, spon- taneous instability	IT	η_{c89}	2.95	295	2030	75.7	34.3	25.7	11.65	218	1500	---	---	
C	11	Basic heat sink	21.6	54.9	1.6	4.07	No pulses, stable	---	93.5	2.91	324	2230	78.1	35.4	26.9	12.2	247	1700	173	1193	
	12	Basic heat sink	21.6	54.9	1.6	4.07	No pulses, stable	IT	93.9	2.95	322	2220	78	35.3	26.4	11.95	245	1690	170	1172	
	13	Basic heat sink	21.6	54.9	1.6	4.07	No pulses, stable	IT	-----	2.61	300	2070	72.6	32.9	27.8	12.6	227	1565	196	1350	Unstable before steady state attained
D	27	Basic heat sink	21.6	54.9	1.6	4.07	No pulses, stable	---	98	2.94	326	2245	75.2	34.1	25.6	11.6	307	2145	219	1510	
	28	Basic heat sink	21.6	54.9	1.6	4.07	No pulses, stable	IT	-----	2.89	313	2160	76.4	34.6	25.5	11.55	321	2210	220	1515	Unstable before steady state attained
	29	Basic heat sink	21.6	54.9	1.6	4.07	No pulses, stable	IT	-----	2.92	311	2140	75.6	34.2	25.8	11.7	321	2210	220	1515	Unstable before steady state attained

54	Basic heat sink	23.4	59.4	---	-----	No pulses, stable	---	-----	316	2180	78.4	35.5	-----	322	2220	---	-----	Fuel flowmeter malfunction
64	Basic heat sink	18.4	46.6	---	-----	No pulses, stable	---	-----	316	2180	73.5	33.3	25.5	11.55	---	-----	---	---
65	Basic heat sink	18.4	46.6	---	-----	No pulses, stable	---	-----	317	2185	74	33.5	25.5	11.55	---	-----	---	---
38	Water-cooled combustor	18.6	47.3	4.1	10.4	27.5 (1.78)	1T	-----	316	2180	73.6	33.4	25.3	11.45	279	1920	178	1227
40	Water-cooled combustor	27.9	70.8	---	-----	No pulses, stable	---	-----	316	2180	74.3	33.6	25.3	11.45	285	1963	172	1850
41	Water-cooled combustor	---	---	---	-----	No pulses, stable	---	-----	314	2165	69.5	31.5	25.8	11.7	246	1695	178	1227
42	Water-cooled combustor	---	---	---	-----	No pulses, stable	---	-----	313	2160	78.7	35.6	24.6	11.15	317	2185	163	1123
43	Water-cooled combustor	---	---	---	-----	No pulses, stable	---	-----	224	1545	52.2	23.6	18.1	8.23	138	950	89	614
44	Water-cooled combustor	---	---	---	-----	No pulses, stable	---	-----	315	2170	74.4	33.7	25.2	11.4	279	1920	170	1172
55	Water-cooled combustor	---	---	---	-----	No pulses, stable	---	-----	315	2170	74.8	33.9	25.1	11.35	---	-----	---	10-sec run
52	Water-cooled combustor and nozzle extension.	17.9	45.5	---	-----	No pulses, stable	---	-----	314	2165	74.3	33.7	25.2	11.4	291	2005	171	1180
53	Water cooled combustor and nozzle extension.	17.9	45.5	---	-----	No pulses, stable	---	-----	313	2160	73.8	33.4	25.5	11.55	288	1985	176	1213
E	14 Basic heat sink	21.6	54.9	1.6	4.07	No pulses, stable	---	-----	306	2110	77.3	35	24.7	11.2	281	1835	137	945
15	Basic heat sink	21.6	54.9	1.6	4.07	No pulses, stable	---	-----	305	2100	77.4	35.1	24.5	11.1	---	-----	---	Chamber pressure tap failure
19	Basic heat sink	31.9	81	1.6	4.07	21.5 (1.39)	1T	-----	---	---	71.6	32.4	28.8	13.05	---	---	---	Chamber pressure tap failure
33	Water-cooled combustor	27.9	70.8	---	-----	No pulses, stable	---	-----	223	1535	53	24	18.8	8.54	139	957	78	537
34	Water-cooled combustor	27.9	70.8	---	-----	No pulses, stable	---	-----	309	2130	74.8	35.5	26	11.8	275	1895	146	1005
F	26 Basic heat sink	16.1	40.9	1.6	4.07	Spontaneous	2T	-----	278	1915	73.7	33.4	25.3	11.45	322	2220	287	1980
G	63 Basic heat sink	21.6	54.9	1.6	4.07	Spontaneous	1T	-----	274	1885	68.5	31	23.1	10.45	222	1530	115	793

^aLength from injector face to nozzle.

^bLength from injector face to centerline of pulse gun barrel.

^cFirst longitudinal, 1L; first tangential, 1T; second tangential, 2T.

^dPerformance during unstable combustion.

^eMinimum charge size loaded for test.

TABLE II. - Concluded. EXPERIMENTAL DATA

In-jector	Run	Combustor configuration	Combustor length ^a		Pulse gun position ^b		Charge information, grain (gram) where applicable	Mode	Characteristic exhaust velocity efficiency, η_{c*}	Oxidant-fuel ratio, O/F	Chamber pressure		Oxidant flow rate		Fuel flow rate		Oxidant injector pressure change		Fuel injector pressure change		Remarks
			in.	cm	in.	cm					psi	KN/m ²	lbm/sec	kg/sec	lbm/sec	kg/sec	psi	KN/m ²	psi	KN/m ²	
B	24	Heat sink combustor with heat sink aperture liner	26.1	54.9	6.1	15.5	No pulses, spontaneous	1T	90.2	2.87	302	2080	71.4	32.3	26.7	12.1	175	1205	179	1235	
C	16	Heat sink combustor with four-spoke heat sink baffle	23.9	60.6	3.8	9.65	Paps and unstained instability	---	95.6	3.02	332	2270	79.7	36.1	26.4	12	248	1710	152	1047	Injector burned-out
C-A	35	Heat sink combustor with water-cooled four-spoke baffle	23.9	60.6	3.8	9.65	Paps	---	93.5	2.91	305	2100	73.4	33.2	25.2	11.4	207	1425	160	1100	
D	20	Heat sink combustor with water-cooled four-spoke baffle	23.9	60.6	3.8	9.65	No pulses, stable	---	-----	1.36	102	703	58.7	26.6	43.3	19.6	142	977	356	2450	Propellant controller malfunction
	21	Heat sink combustor with water-cooled four-spoke baffle	23.9	60.6	3.8	9.65	30.5 (1.98)	(f)	-----	2.92	---	---	73.4	33.2	25.1	11.4	---	---	---	---	Chamber pressure tap failure
	30	Heat sink combustor with water-cooled silt liner	26.9	68.3	6.8	17.3	Stable to 39 (2.53)	---	97.5	2.97	308	2120	71.3	32.3	24	10.9	275	1895	171	1176	
	31		26.9	68.3	6.8	17.3	Stable to 39 (2.53)	---	97.6	2.92	318	2190	73	33.1	25	11.3	281	1935	178	1225	
	32		21.9	55.6	6.8	17.3	Stable to 39 (2.53)	---	96.1	3.01	312	2150	74	33.5	24.6	11.2	301	2070	178	1225	
	56		18.9	48	4.3	10.9	No pulses, stable	---	97.2	2.99	315	2170	75.1	34.1	25.1	11.4	---	---	169	1165	
	57		23.9	60.6			Stable to 36.5 (2.37)	---	97.4	2.96	317	2180	73.8	33.4	24.9	11.3	287	1975	164	1130	Largest charge used in test
	58		23.9	60.6			Stable to 36.5 (2.37)	---	97	2.97	318	2190	74.4	33.7	25	11.3	254	1747	---	---	Largest charge used in test
	59		23.9	60.6			Spontaneous	1T	$d_{89.2}$	2.98	306	2110	78.1	35.4	26.2	11.9	335	2310	209	1440	
E	47	Heat sink combustor with water-cooled silt liner	21.4	54.4	6.8	17.3	Stable to 39 (2.53)	---	92.3	2.88	304	2100	74.4	33.7	25.8	11.7	273	1880	148	1020	
	48							---	92.2	2.87	304	2100	74.1	33.6	25.9	11.75	273	1880	155	1067	
	49							---	91.9	2.90	302	2080	74.4	33.7	25.6	11.6	272	1875	147	1010	
	50							---	92.1	2.90	299	2060	73.4	33.2	25.3	11.45	270	1860	146	1005	

^aLength from injector face to nozzle.^bLength from injector face to centerline of pulse gun barrel.^cFirst longitudinal, 1L; first tangential, 1T; second tangential, 2T.^dPerformance during unstable combustion.^f3040 Hz.

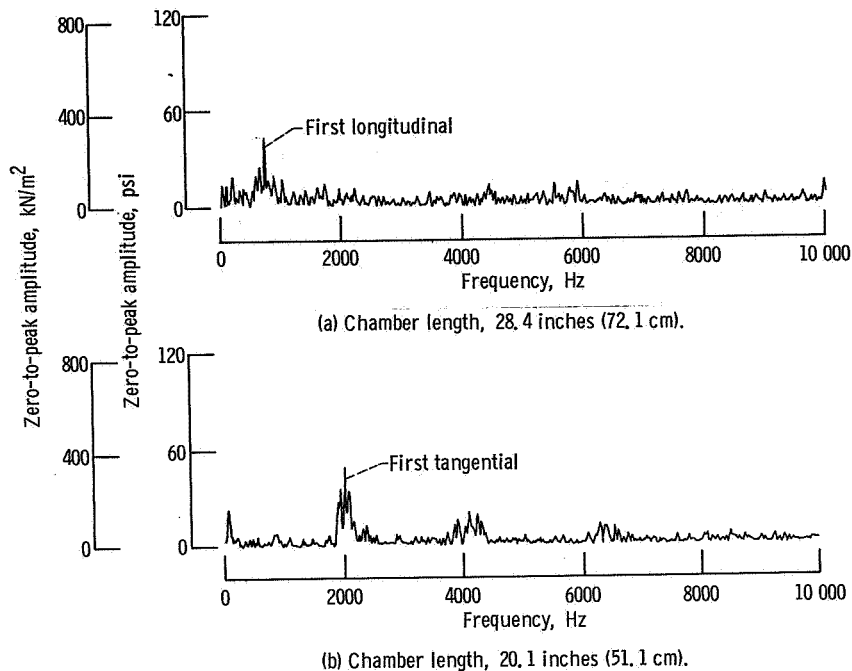


Figure 7. - Typical amplitude spectral density plots for injector A.

In a 28.4-inch (72.1-cm) length thrust chamber (measured from the injector face to the nozzle throat), the injector was still spontaneously unstable in the first longitudinal acoustic mode at an oscillation frequency of about 750 hertz. As seen in figure 7(a) the amplitude of the oscillation was about 50 psi (345 kN/m^2) (zero-to-peak). When decreased to 20.1 inches (51 cm) in length, the combustor was still spontaneously unstable, but caused a change in the predominant mode from first longitudinal to first tangential (fig. 7(b)). The frequency of the oscillation was about 2000 hertz with an amplitude of about 50 psi (345 kN/m^2) (zero-to-peak).

It should be noted that the values of characteristic exhaust velocity efficiency presented in table II for this injector were necessarily calculated for operation during unstable combustion.

A postfiring photograph of the injector after a total of 8.2 seconds in seven separate tests is shown in figure 3(a). Other than missing 47 of the 268 tube extensions due to mechanical failure, the injector face plate and tube extensions did not suffer any damage.

Injector configuration B: like-on-like doublet with intersecting fans. - This configuration had 387 oxidant doublet elements and 129 fuel doublet elements. The element arrangement is shown in figure 3(b). In the course of the program, the injector was modified by closing-off the 129 oxidant doublet elements which impinged beneath the fuel doublets. This was an attempt to provide more stability by decreasing interfacial liquid-phase reactions. Studies of reference 7 observed that interfacial reactions cause uneven distribution of oxidant and fuel droplets which can lead to combustion instability.

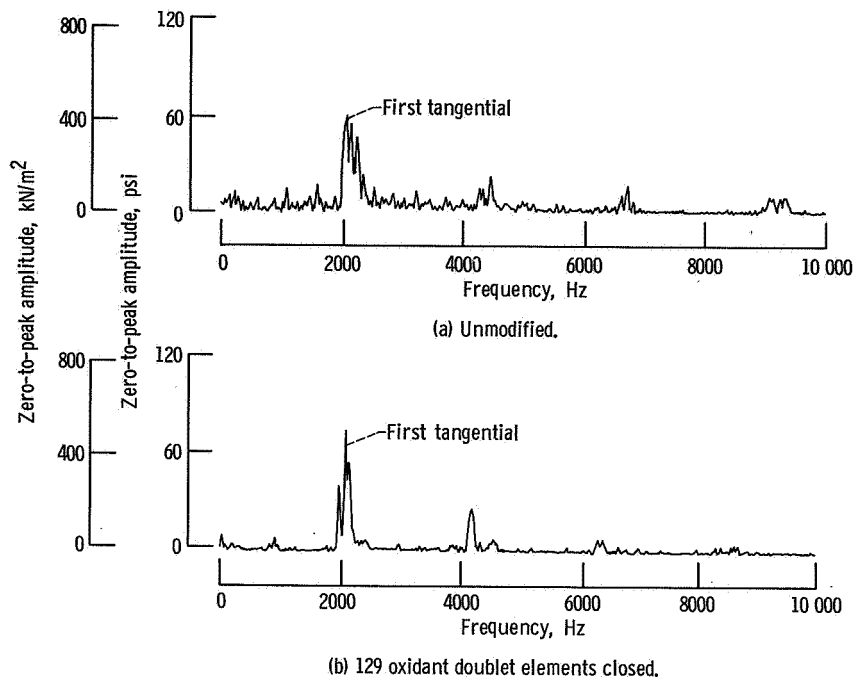


Figure 8. - Typical amplitude spectral density plots for injector B.

Both injector configurations were evaluated in 21.6-inch (54.9-cm) length thrust chambers. The stability characteristics of the injectors appeared to be the same (fig. 8); both were spontaneously unstable in the first tangential mode. The amplitude of the oscillation in both cases reached values between 60 to 80 psi (413 to 551 kN/m^2) zero-to-peak.

Injector configuration C: like-on-like doublet with nonintersecting fans. - The injector had 144 oxidant doublet elements, four oxidant shower-head elements and 52 fuel doublet elements. The elements were arranged in groups of three and in an orientation to produce three parallel fans with the fuel in the center (fig. 3(c)). This particular arrangement was the most stable configuration of all the injectors tested in the small scale investigation of reference 2. Twenty oxidizer doublets and four shower-head elements were distributed around the periphery of the injector face in an attempt to eliminate void areas where pockets of propellant could concentrate and possibly detonate.

Three tests were conducted with the configuration in a 21.6-inch (54.9-cm) length thrust chamber. In all tests, the combustor was statically stable. The combustor did not, however, provide any margin of dynamic stability. A charge size of only $21\frac{1}{2}$ grains (1.39 grams) of nitrocellulose triggered the first tangential mode of sustained instability. Smaller gun charges were not fired because the stability margin was not considered adequate unless the combustor could damp charges of 35 to 40 grains (2.27 to 2.59 grams) of nitrocellulose. This stability criterion was purely arbitrary. Prior to this investigation, the minimum gun charge size that triggered instability in any investigation at the Center had been about 35 grains (2.27 grams). The amplitude of the oscillation was

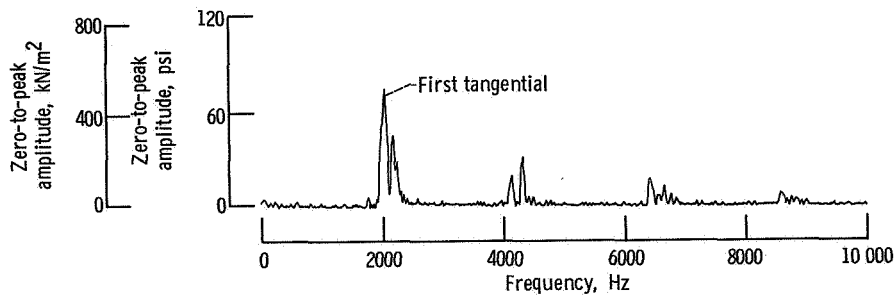


Figure 9. - Typical amplitude spectral density plot for injector C.

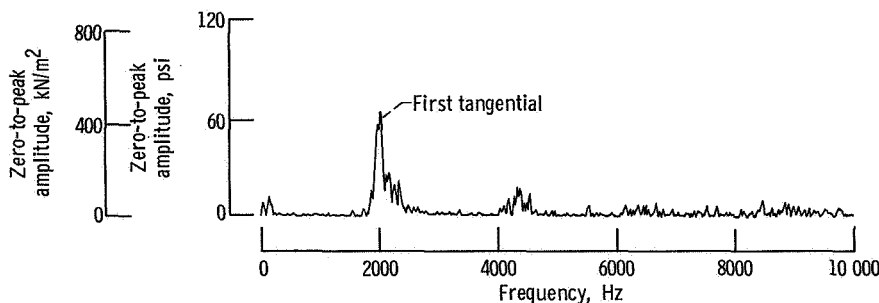


Figure 10. - Typical amplitude spectral density plot for injector D.

about 70 psi zero-to-peak (482 kN/m^2) (fig. 9). The characteristic exhaust velocity efficiency of the combustor varied from $93\frac{1}{2}$ to 94 percent of theoretical equilibrium.

Injector configuration D: like-on-like doublet with nonintersecting fans. - Basically, this configuration was a fine pattern version of injector configuration C. The injector had 252 oxidant doublet elements, 96 fuel doublet elements, and 32 fuel shower-head elements (fig. 3(d)). The 32 fuel shower-head elements were distributed around the periphery of the injector to eliminate void areas.

A total of 15 tests were conducted with this injector configuration in thrust chambers (both cooled and uncooled) that varied in length from 17.9 to 27.9 inches (45.5 to 70.9 cm). Several tests were conducted at off-design conditions of oxidant-fuel ratio and chamber pressure. In every test, the combustor was statically stable, however, similar to configuration C, the combustor did not provide an adequate margin of dynamic stability. Pulsing the combustor approximately 1.6 inches (4.07 cm) downstream of the injector face with $18\frac{1}{2}$ grains (1.2 grams) of nitrocellulose triggered the first tangential mode. The amplitude of the oscillation was 70 psi (482 kN/m^2) (zero-to-peak) and the frequency of the oscillation was about 2000 hertz (fig. 10).

As expected, the performance of this injector was higher than configuration C. As shown in figure 11, the characteristic exhaust velocity efficiency was $96\frac{1}{2}$ percent at an oxidant fuel ratio of 3 and increased to about 98 percent as the oxidant-fuel ratio was

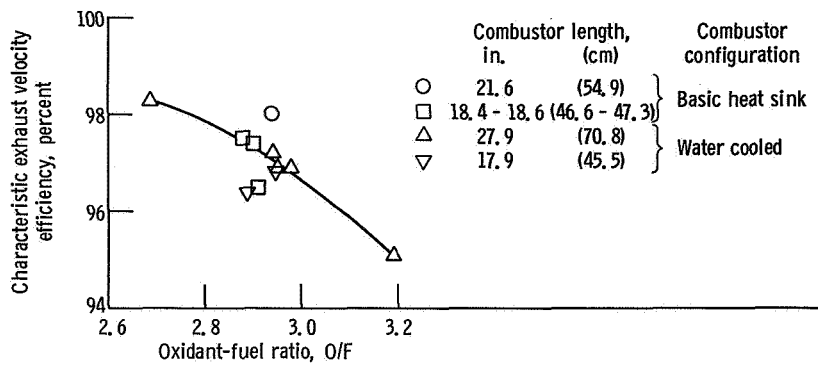


Figure 11. - Statically stable combustion performance of combustors with injector D. Basic combustor chamber pressure, nominally 300 psi (2070 kN/m²).

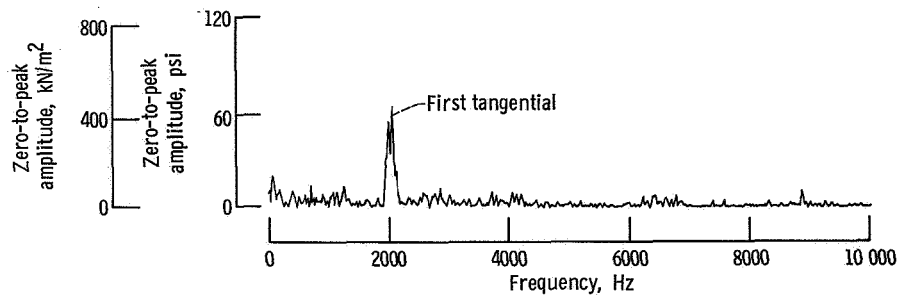


Figure 12. - Typical amplitude spectral density graphs for injector E.

decreased to 2.7. Any effect of varying combustor length from 27.9 to 17.9 inches (70.9 to 45.5 cm) on combustor performance was not apparent in these results.

Injector configuration E: like-on-like fuel doublet and oxidant shower-head element combination. - The injector consisted of 980 shower-head oxidizer elements and 96 fuel doublet elements (fig. 3(e)). The element orientation was such that the resultant fuel fans were perpendicular to the row of shower-head elements, thus, producing impingement of unlike propellants. Based on the previous results, it appeared that this injector would have poor stability characteristics, however, as seen in table II the configuration was statically stable in all five tests conducted with this injector and the basic combustor. The stability margin was low, requiring a charge size of only $21\frac{1}{2}$ grains (1.39 grams) (smallest charge evaluated with this injector) to trigger the first tangential mode of instability. The amplitude of the oscillation was about 70 psi (482 kN/m²) (zero-to-peak) (fig. 12).

The combustion performance of the injector in a 21.6-inch (54.9-cm) length combustor was 92 percent of equilibrium characteristic exhaust velocity. Increasing the combustor length to 27.9 inches (70.9 cm), increased the performance about 1 percentage point to 93 percent (table II). However, the 27.9-inch (70.9-cm) length combustor was

water cooled, so precise performance comparison cannot be made because of the difference in heat loss to the chamber.

Injector configuration F: pentad and triplet element combination. - The injector consisted of 188 oxidant-on-fuel pentad elements and 112 oxidant-on-fuel triplet elements (fig. 3(f)). The injector, which was statically stable with 50-percent UDMH - 50-percent N_2H_4 and nitrogen tetroxide at an oxidant-fuel ratio of 2 or below, was an existing configuration from an ablative engine investigation. The element arrangement was basically a grid pattern of pentad elements surrounded by three circumferential rows of triplets to provide uniform combustion near the walls of the combustor for better ablative compatibility.

With hydrazine and nitrogen tetroxide propellants the configuration was spontaneously unstable. The mode of instability was more complex than observed with the other combustors and contained two frequencies of 2500 and 3500 hertz. The amplitude of the predominant oscillation (3500 Hz) was about 90 psi (620 kN/m^2) (fig. 13). Only one test was conducted with the injector because during the test the chamber pressure transducer line failed, allowing combustion gas to escape and resulted in a burnout of the face plate (fig. 3(f)).

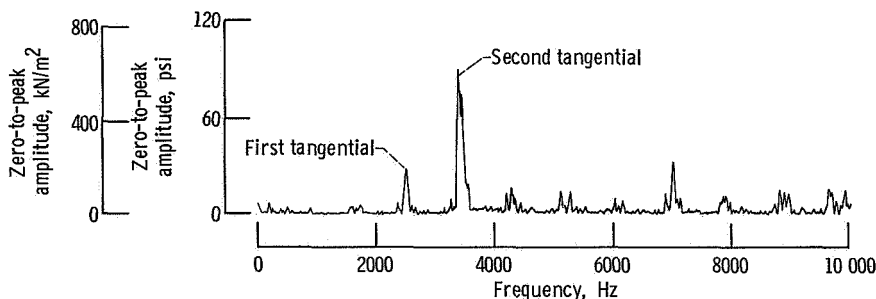


Figure 13. - Typical amplitude spectral density graph for injector F.

Injector configuration G: 101 element fuel-oxidant-fuel triplet injector. - This injector was also an existing configuration used in a 50-percent UDMH - 50-percent N_2H_4 and N_2O_4 propellant combination acoustic-mode instability investigation. The injector incorporated rectangular injection orifices in 55 of the 101 elements (in selected radial regions) in an attempt to provide increased stability through increased propellant stream hydraulic rigidity to tangential or radial pressure oscillations (fig. 3(g)). With the 50-percent UDMH - 50-percent N_2H_4 and N_2O_4 propellant combination, the injector was statically stable in only three of five tests.

Prior to testing the injector with hydrazine and nitrogen tetroxide propellants, the injector was modified in an attempt to improve tangential mode stability by providing a nonuniform or "hump" mass flux propellant radial distribution (ref. 8). The circular

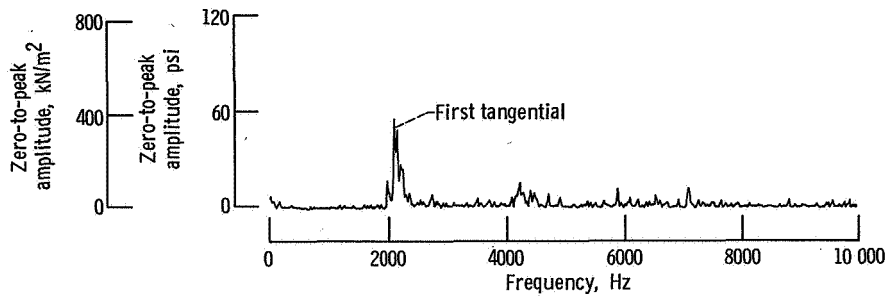


Figure 14. - Typical amplitude spectral density graph for injector G.

orifice elements which were located at about $1/2$ chamber radius were drilled out so that 60 percent of the total flow would pass through these elements. Several tests were conducted with the injector using hydrazine and nitrogen tetroxide and all were spontaneously unstable. The mode of instability was first tangential with a zero-to-peak amplitude of 60 psi (413 kN/m^2) (fig. 14).

In summary most of the injectors were not statically stable and none was stable to a $21\frac{1}{2}$ grain (1.39 grams) charge (1.6 in. or 4.07 cm from injector). Since more dynamic stability was desirable a few tests were conducted using acoustic liners and baffles. The results of these tests are reported in the following section.

STABILITY CHARACTERISTICS OF INJECTORS WITH ACOUSTIC LINERS AND BAFFLES

The tests with acoustic liners and baffles were limited to only the three injector configurations (C, D, and E) that were statically stable but dynamically unstable.

The liner configurations tested included a four-row, circular aperture liner (fig. 5(a)) and a circumferential slot liner (fig. 5(b)). The calculated absorption coefficient (defined as the percent of the total incident energy damped by the liner) curves for each half of the four-row, circular aperture liner are presented in figures 15(a) and (b). The curves were calculated for an assumed sound pressure level of 190 decibels, an assumed velocity past the apertures of 1200 feet per second (366 m/sec), and for three assumed liner cavity gas temperatures of 1440° , 1980° , and 2520° R (800, 1100, and 1400 K). The first two rows from the injector (fig. 15(a)) were tuned for a frequency between 3500 and 4500 hertz and the last two rows for a frequency between 1800 to 2400 hertz (fig. 15(b)) with the assumed cavity gas temperatures. Absorption characteristic curves for the slot liner at the same cavity gas temperatures and sound pressure level are shown in figure 16. Depending on the cavity gas temperature, the resonant frequency of the liner varied between 2300 and 3000 hertz.

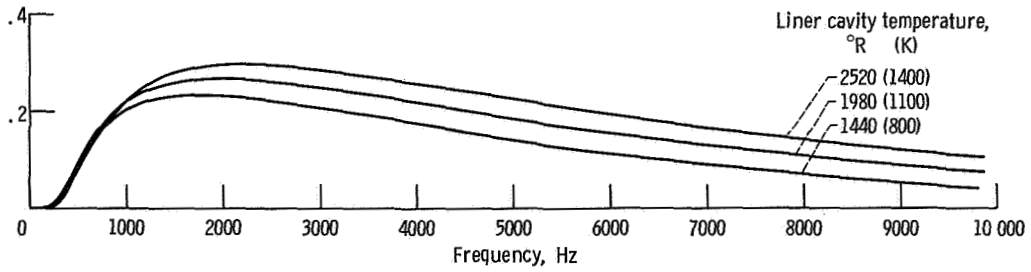
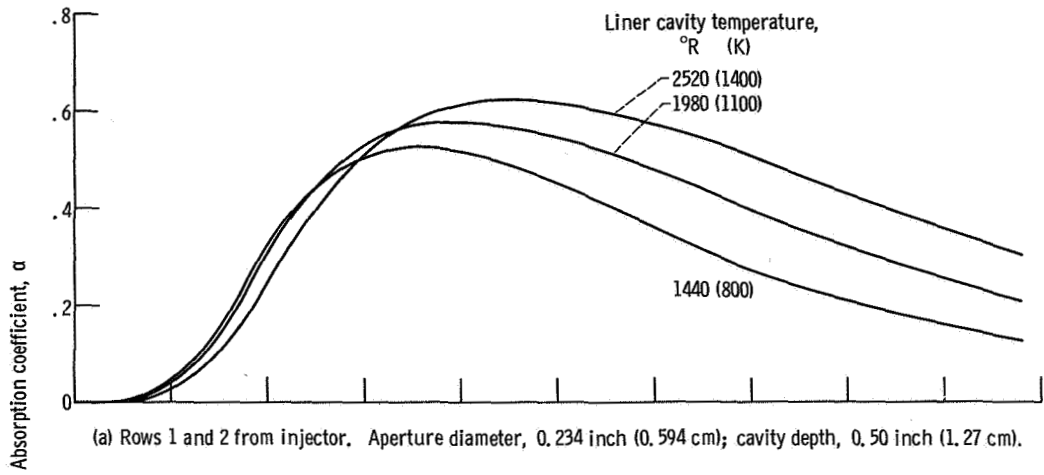
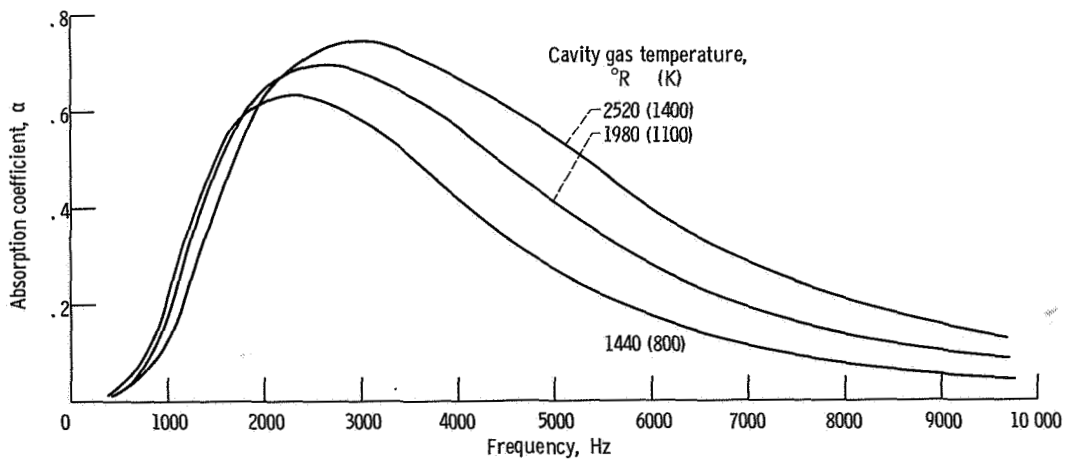


Figure 15. - Circular aperture liner absorption characteristics. Liner thickness, 0.34 inch (0.864 cm); velocity past, 1200 feet per second (366 m/sec).



Because most of the injectors investigated were existing configurations not designed to accommodate face baffles, the tests were limited to the four-spoke configuration, the design most compatible with the element pattern. The baffle length selected (2.25 in. or 5.72 cm) was based on studies reported in reference 9.

Injector configuration C. - With either the four-spoke baffle or the four-row, circular aperture liner (slot liner was not tested with this injector), the combustor damped all pulses to the limiting charge size of 39 grains (2.53 grams) of nitrocellulose (limited by cartridge volume). Combustion with the baffle, however, was not satisfactory because a "popping" type of instability was present throughout the tests. The instability (popping) was initially thought to be associated with the uncooled baffle and the gap between the baffle and injector faceplate. However, later tests with a water-cooled baffle configuration which was sealed to the injector faceplate proved this hypothesis to be in error. Postfiring inspection revealed slight erosion patterns on the faceplate where the baffle legs intersected the chamber wall. The erosion may indicate that concentrations of propellant detonated or "popped" in these areas.

Testing with the four-row, circular-aperture, water-cooled liner was limited to only one test because an irreparable water leak developed in an O-ring seal. The liner cavity gas temperatures, which are plotted in figure 17, were found to be higher than the range of values used in the design. After about 2-second firing duration, the cavity temperatures approached values between 2750° and 3250° R (1530 and 1800 K). Assuming an average cavity gas temperature of 3000° R (1667 K), the calculated resonant frequency of the first two rows of apertures was 5000 hertz and the last two rows was 2200 hertz. Because of the broad absorption frequency bandwidth characteristics of the design, this

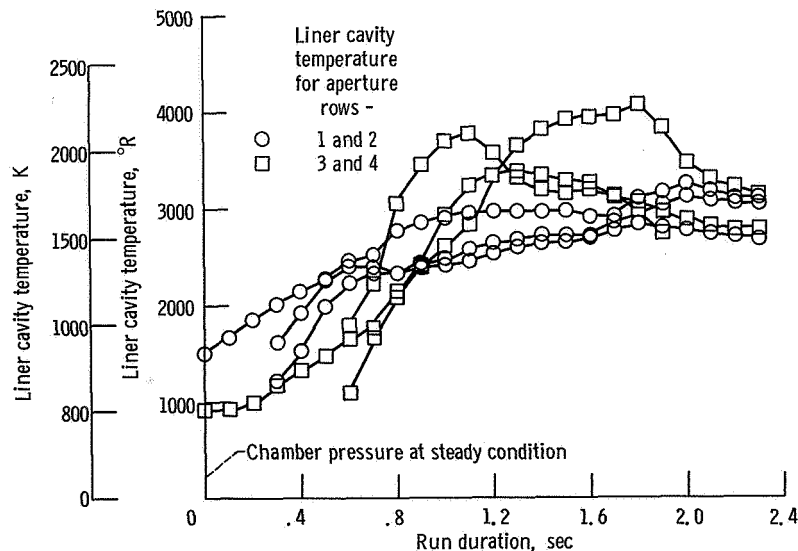


Figure 17. - Four row, circular aperture cavity gas time history.

temperature variance from the design values did not grossly affect the performance of the liner. The calculated absorption coefficient for the first two rows of holes (at a frequency of 3500 Hz) was 0.58 and the last two rows of holes (at a frequency of 2000 Hz) was 0.32.

Injector configuration D. - Tests evaluating the stability characteristics of this injector and the four-spoke baffle were completely free of any popping type of instability. The screech stability margin, however, was only slightly improved by the baffle. With the baffle, a pulse size of $30\frac{1}{2}$ grains (1.98 grams) of nitrocellulose was required to trigger instability compared with $27\frac{1}{2}$ grains (1.78 grams) without the baffle. As mentioned earlier, the change in the baseline stability from less than $18\frac{1}{2}$ to $27\frac{1}{2}$ grains (1.2 to 1.78 grams) of nitrocellulose is due to moving the location of the pulse gun about $2\frac{1}{2}$ inches (6.35 cm) further downstream.

The circumferential slot liner improved the dynamic stability margin of the injector to pulse gun charges of over 39 grains (2.53 grams) (maximum possible) when fired immediately downstream of the liner. In the final test of the configuration, however, combustion was unstable. This was attributed to a spontaneous pressure pop which had an amplitude of greater magnitude than that possible with the pulse gun. The pop was believed due to detonation of the fuel in an annular crack which existed on the upstream side of the chamber section containing the liner. The crack was due to flange warpage during liner fabrication and had been sealed with a rubber compound during engine assembly. A postfiring inspection, however, revealed that all the sealant was missing leaving a 1/32-inch (1.79-mm) width crack between the liner section and the injector face. Typical liner cavity gas temperature time histories are presented in figure 18. The large variation in temperature (from 2000° to 3250° R or 1110 to 1800 K) between two diametrically opposite thermocouples is not understood. As far as could be determined,

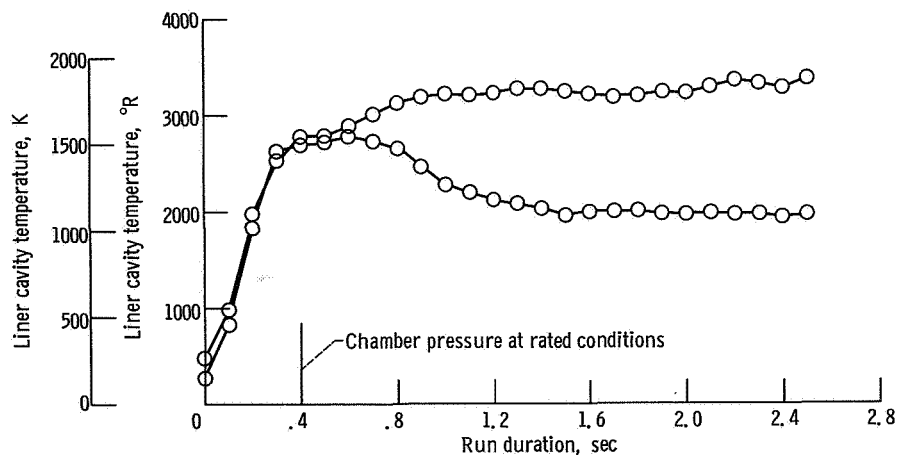


Figure 18. - Slit liner cavity gas time history.

the effect did not appear to be associated with the installation or injector element pattern. The calculated absorption coefficients for the liner at cavity gas temperatures of 2000° and 3250° R (1110 to 1850 K) and a frequency of 2000 hertz were 0.65 and 0.58, respectively.

Injector configuration E. - Because of marginal success of the four-spoke baffle, and a structural failure of the four-row, circular aperture liner (in previous tests), the tests with this injector were limited to only the circumferential slot liner. The liner configuration was again very effective in improving stability characteristics. The combustor successfully damped pulse gun charges of 39 grains (2.53 grams) of nitrocellulose. (Note that the pulse gun was again located further downstream in this configuration than in the bare chamber configuration.) Combustion was also free of any popping type of instability in all four tests. Liner cavity gas temperatures were not obtained for the tests because of instrument malfunction.

CONCLUDING REMARKS

Of the seven different injector configurations tested, only configurations C, D, and E were statically stable and none were dynamically stable to a $21\frac{1}{2}$ grain (1.39 gram) charge. Injectors C and D had like-on-like doublet elements with nonintersecting fans while injector E had like-on-like doublet fuel elements and shower-head oxidizer elements. All other injectors utilized injection schemes with unlike propellant impingement or like-on-like doublets with intersecting fans. Based on the results of this study, it is therefore concluded that for the best stability with the highly reactive, hypergolic propellants of hydrazine and nitrogen tetroxide (at an oxidant-fuel ratio of 3) an injector with like-on-like doublets with nonintersecting fans should be used. The fact that all of the unlike impingement type injectors had previously been statically stable with 50-percent UDMH - 50-percent N_2H_4 and N_2O_4 suggests that the initiating mechanism of acoustical mode instability is associated with the reactivity of the propellant combination. Interfacial reaction (or jet blow apart) with the more reactive propellant combination, N_2H_4 - N_2O_4 , (ref. 10) could cause local N_2H_4 concentrations which might react as a monopropellant. Such monopropellant reaction would tend to propagate the shock front of the combustion instability.

Injector configuration D, which had the highest combustion performance in addition to being statically stable, was selected for use in the hypersonic combustion investigation.

SUMMARY OF RESULTS

Performance and stability characteristics of seven different injectors utilizing injection types of like-on-like doublet elements, combination of like-on-like doublet elements and shower-head elements, oxidant-fuel-oxidant triplets and a combination of pentad and triplet elements were investigated. Since the combustors were to be used as hot gas generators in a hypersonic combustion facility, the tests were limited to an oxidant-fuel ratio of 3 at which the exhaust products simulate the gas composition of air. Chamber pressure was 300 psia (2070 kN/m^2) nominal. The investigation yielded the following results:

1. Injectors with like-on-like doublet elements with parallel fans for both propellants or a combination of like-on-like fuel doublet elements and shower-head oxidizer elements were the only configurations that were statically stable.

2. The statically stable injectors had little dynamic stability, requiring only about 20 grains (1.3 grams) of nitrocellulose to induce instability.

3. High performance was achieved with like-on-like doublet element injectors. Injector configuration D had a characteristic exhaust velocity efficiency of $96\frac{1}{2}$ percent at an oxidant-fuel ratio of 3 in an 18-inch (46-cm) length combustor.

4. A four-spoke, $2\frac{1}{4}$ -inch (5.72-cm) length baffle provided only a slight improvement in stability margin.

5. Both the circumferential slot liner, and four-row circular aperture liner improved the stability margin of the statically stable injectors to a pulse size of over 39 grains (2.53 grams) of nitrocellulose (largest charge possible).

Lewis Research Center,

National Aeronautics and Space Administration,

Cleveland, Ohio, April 23, 1969,

722-03-00-04-22.

REFERENCES

1. Metzler, A. J.; and Lezberg, E. A.: A Hot Gas Generator for Large Scale Supersonic Combustor Testing. Paper 68-647, AIAA, June 1968.
2. Hersch, Martin: Performance and Stability Characteristics of Nitrogen Tetroxide-Hydrazine Combustors. NASA TN D-4776, 1968.
3. Sokolowski, Daniel E.; Vincent, David W.; and Conrad, E. William: Characterization of Pressure Perturbations Induced In a Rocket Combustor by a Machine Gun. NASA TN D-5214, 1969.

4. Phillips, Bert; Hannum, Ned P.; and Russell, Louis M.: On the Design of Acoustic Liners for Rocket Engines: Helmholtz-Resonators Evaluated with a Rocket Combustor. NASA TN D-5171, 1969.
5. Van Itterbeek, A.; Van Engelen, H.; and Myncke, H.: Influence of the Shape of the Neck of the Helmholtz-Resonator on its Absorbing Properties. *Acoustica*, vol. 14, no. 4, 1964, pp. 212-215.
6. Vincent, David W.; Phillips, Bert; and Wanhainen, John P.: Experimental Investigation of Acoustic Liners to Suppress Screech in Storable Propellant Rocket Motors. NASA TN D-4442, 1968.
7. Burrows, Marshall C.: Hydrazine - Nitrogen Tetroxide Combustion Response to Transverse Gas Flows. Presented at the Fifth ICRPG Combustion Conference, Howard County, Md., Oct. 1-3, 1968.
8. Reardon, F. H.; McBride, J. M.; and Smith, A. J., Jr.: Effect of Injection Distribution on Combustion Stability. *AIAA J.*, vol. 4, no. 3, Mar. 1966, pp. 506-512.
9. Vincent, David W.; Sokolowski, Daniel E.; and Bloomer, Harry E.: Screech Suppression Techniques for Rocket Combustors Using Earth-Storable Propellants. NASA TM X-1595, 1968.
10. Feiler, Charles E.; and Baker, Louis, Jr.: A Study of Fuel-Nitric Acid Reactivity. NACA RM E56A19, 1956.

NATIONAL AERONAUTICS AND SPACE ADMINISTRATION
WASHINGTON, D. C. 20546
OFFICIAL BUSINESS

FIRST CLASS MAIL



POSTAGE AND FEES PAID
NATIONAL AERONAUTICS AND
SPACE ADMINISTRATION

POSTMASTER: If Undeliverable (Section 158
Postal Manual) Do Not Return

"The aeronautical and space activities of the United States shall be conducted so as to contribute . . . to the expansion of human knowledge of phenomena in the atmosphere and space. The Administration shall provide for the widest practicable and appropriate dissemination of information concerning its activities and the results thereof."

— NATIONAL AERONAUTICS AND SPACE ACT OF 1958

NASA SCIENTIFIC AND TECHNICAL PUBLICATIONS

TECHNICAL REPORTS: Scientific and technical information considered important, complete, and a lasting contribution to existing knowledge.

TECHNICAL NOTES: Information less broad in scope but nevertheless of importance as a contribution to existing knowledge.

TECHNICAL MEMORANDUMS: Information receiving limited distribution because of preliminary data, security classification, or other reasons.

CONTRACTOR REPORTS: Scientific and technical information generated under a NASA contract or grant and considered an important contribution to existing knowledge.

TECHNICAL TRANSLATIONS: Information published in a foreign language considered to merit NASA distribution in English.

SPECIAL PUBLICATIONS: Information derived from or of value to NASA activities. Publications include conference proceedings, monographs, data compilations, handbooks, sourcebooks, and special bibliographies.

TECHNOLOGY UTILIZATION PUBLICATIONS: Information on technology used by NASA that may be of particular interest in commercial and other non-aerospace applications. Publications include Tech Briefs, Technology Utilization Reports and Notes, and Technology Surveys.

Details on the availability of these publications may be obtained from:

SCIENTIFIC AND TECHNICAL INFORMATION DIVISION
NATIONAL AERONAUTICS AND SPACE ADMINISTRATION
Washington, D.C. 20546